$\mathbb{Z}_2$ spin liquid and chiral antiferromagnetic phase in the Hubbard model on a honeycomb lattice

Yuan-Ming Lu and Ying Ran
Department of Physics, Boston College, Chestnut Hill, MA 02467, USA
(Received 5 December 2010; revised manuscript received 4 April 2011; published 15 July 2011)

In a Schwinger-fermion representation we classify all 128 possible spin liquids that preserves $SU(2)$ spin-rotational symmetry, honeycomb lattice group symmetry, and time-reversal symmetry. Among them we identify a Z_2 spin liquid called the sublattice-pairing state (SPS) as the spin liquid phase discovered in recent numerical study on a honeycomb lattice [Meng *et al.*, Nature (London) **464**, 847 (2010)]. Our method provides a systematic way to identify spin liquids close to Mott transition. We also show that the SPS is identical to the zero-flux Z_2 spin liquid in Schwinger-boson representation [Wang, Phys. Rev. B **82**, 024419 (2010)]. through an explicit duality transformation. SPS is connected to an *unusual* antiferromagnetic ordered phase, which we term the chiral-antiferromagnetic (CAF) phase, by an $O(4)$ critical point. The CAF phase breaks the $SU(2)$ spin rotational symmetry completely and has three Goldstone modes. Our results indicate that there is likely a hidden phase transition between the CAF phase and the simple antiferromagnetic phase at large U/t. We also propose numerical measurements to reveal the CAF phase and the hidden phase transition.

DOI: 10.1103/PhysRevB.84.024420 PACS number(s): 75.10.Kt, 71.27.+a

I. INTRODUCTION

A novel state of matter, a quantum spin liquid (SL), has been recently discovered in organic spin-1/2 triangular lattice experimental systems.[1–3] This class of organic Mott insulators is in the vicinity of the Mott transition and can be driven into a Fermi liquid by applying pressure. A quantum SL is the ground state of a Mott insulator which does not break physical symmetries, and cannot be adiabatically connected to a band insulator. After Anderson's proposal of resonating-valence-bond (RVB) states,[4] a lot of theoretical and experimental efforts have been made to show the existence of such novel phases of matter with fractionalized excitations.[5] For example, various exact or quasi-exact solvable models[6–9] hosting SL ground states have been constructed. The exciting experimental progress on the triangular lattice organics raises an interesting question: Can a SL be naturally realized in a Mott insulator close to the Mott transition?[10,11] If this is true, it can serve as a guideline in searching SLs in experimental systems. Physical intuition suggests this is likely to be the case because, in the neighborhood of the Mott transition, quantum fluctuations of spins are strong which can suppress the classical spin ordering.

A recent remarkable numerical study[12] for the nearest neighbor Hubbard model on the honeycomb lattice,

$$H = -t \sum_{\langle ij\rangle\sigma} c^\dagger_{i\sigma} c_{j\sigma} + U \sum_i c^\dagger_{i\uparrow} c_{i\uparrow} c^\dagger_{i\downarrow} c_{i\downarrow}, \qquad (1)$$

provides another price of evidence of this guideline, where an insulating phase respecting all physical symmetry is found in the neighborhood of the Mott transition. This phase has attracted some theoretical attention[13,14] because it cannot be explained as a band insulator due to the honeycomb lattice structure. It should be a SL with fractionalized excitations. There are many different SLs on the honeycomb lattice, characterized by different topological orders.[15] Which SL is realized in the simulated Hubbard model? And in a general context, is there a systematic way to identify the SLs in the neighborhood of a Mott transition? We provide our answers to these questions in this paper.

In Ref. 12, it is shown that this SL phase has a full energy gap and is likely to be smoothly connected (i.e., through a continuous phase transition) to both the semimetal phase for small U/t and an antiferromagnetic (AF) phase for large U/t. These three conditions strongly restrict the candidate SL phases.

There have been two popular approaches to describe SL phases: Schwinger-fermion[16–19] and Schwinger-boson,[6,20] in which the low-energy spin excitations are fermionic and bosonic spinons, respectively. The fermionic approach is more natural to be used in the vicinity of a continuous Mott transition, whereas the bosonic model is more natural when close to a magnetic transition. (This is because, close to a Mott transition, physically the low energy spinons should be the electrons which lose their charge coherence. Bosonic spinon condensation can easily explain the transition into a magnetic ordered phase.) The possible underlying relation between the two seemingly very different approaches has been a long-standing puzzle.

In Schwinger-fermion representation, we classify all possible 128 different Z_2 SLs using a projective symmetry group (PSG).[15] In the vicinity of the Mott transition in the simulated Hubbard model,[12] we will show that there is only one natural SL among them, a Z_2 state coined the sublattice pairing state (SPS) which has a full energy gap and can be smoothly connected to the semimetal phase. Moreover, the Schwinger-boson method has been used to describe the magnetic phase transition[2] in the same system. It was found that only one SL phase, the zero-flux state, can be smoothly connected to an AF ordered phase. The zero-flux state is also a Z_2 state with a full energy gap. However, it is not clear whether this zero-flux state can be smoothly connected to the semimetal phase. Can the SPS be related to the zero-flux state? In this paper, we will demonstrate that, remarkably, the SPS and zero-flux state are identical by an explicit duality transformation in the low-energy effective theory. This is the first identification of a state in both the Schwinger-fermion and the Schwinger-boson methods.

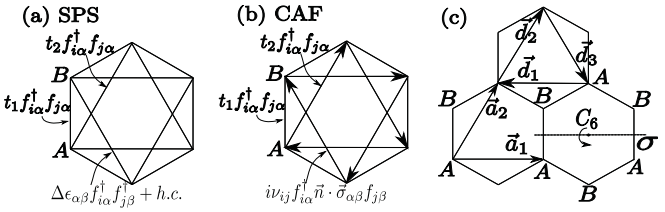

FIG. 1. Mean-field ansatz of (a) SPS phase and (b) CAF phase in terms of the f-fermion. $v_{ij}=1$ if $i\to j$ is along the arrow direction. (c) The honeycomb lattice and its Bravais lattice vector $\vec{a}_{1,2}$. $\vec{d}_{1,2,3}$ are the three vectors used in Eq. (21). Two, generators of the symmetry group are also shown: 60° rotation of C_6, the horizontal mirror σ.

We will also show that the magnetically ordered phase connected to the SPS is rather unusual and *not* the simple Néel phase, because it breaks the SU(2) spin-rotation symmetry completely and has three Goldstone modes. We name this phase the chiral-antiferromagnetic (CAF) phase. Aside from the usual AF spin order parameter $\vec{N}=(-1)^{i_s}\vec{S}_i$, where $i_s=0,1$ for A and B sublattices, respectively, in the CAF phase there is another vector-chirality spin order parameter $\vec{n}=\sum_{\langle\langle ij\rangle\rangle}v_{ij}\vec{S}_i\times\vec{S}_j$, whose expectation value satisfies $\langle\vec{n}\rangle\perp\langle\vec{N}\rangle$. $v_{ij}=+1(-1)$ if one goes from site i to j in a clockwise (counterclockwise) manner, as shown by the arrows in Fig. 1(b). Since the usual AF phase should exist in the large U/t limit,[21] our results suggest a hidden phase transition, which might happen in the "Néel" phase of the previously mentioned numerical study[12] or at a larger U/t not studied before. We therefore propose the schematic phase diagram as shown in Fig. 2(a).

This paper is organized in the following way. In Sec. II we give a brief exposition of the SU(2) Schwinger-fermion approach to SL states and PSG classification of different SLs. Following the mathematical classification of all Z_2 spin liquids using the PSG in Appendix B, we discuss the possible gapped Z_2 SLs continuously connected to a semimetal phase in Sec. III. We find there is only one natural candidate, the SPS. A mean-field study of the SPS in the J_1-J_2 Heisenberg model is given in Appendix F. In Sec. IV we discuss the continuous phase transition between the SPS and a magnetically ordered phase and reveal a hidden order parameter of this CAF phase aside from Néel order parameter. In Sec. V we identify our SPS with the zero-flux state in Schwinger-boson mean-field approach[2] through an explicit duality transformation. Finally, we summarize our results in Sec. VI.

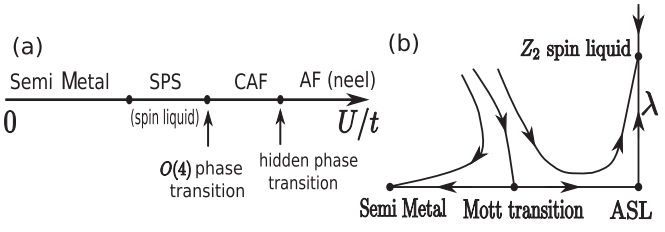

FIG. 2. (a) Proposed schematic phase diagram of the Hubbard model on the honeycomb lattice. (b) Schematic RG flow of the Mott transition.

II. SCHWINGER-FERMION APPROACH AND PROJECTIVE SYMMETRY GROUP

In the large-U limit at half-filling, the charge flucutation in Hubbard model (1) is severely suppressed and the low-energy spin fluctuations are described by the $S=1/2$ Heisenberg model:[43]

$$H_{spin}=-\frac{4t^2}{U}\sum_{\langle ij\rangle}\mathbf{S}_i\cdot\mathbf{S}_j+O\left(\frac{t^3}{U^2}\right). \tag{2}$$

In the Schwinger-fermion approach, a spin-1/2 operator at site i is represented by

$$\vec{S}_i=\tfrac{1}{2}f^\dagger_{i\alpha}\vec{\sigma}_{\alpha\beta}f_{i\beta}. \tag{3}$$

A Heisenberg spin Hamiltonian $H=\sum_{\langle ij\rangle}J_{ij}\vec{S}_i\cdot\vec{S}_j$ is represented as $H=\sum_{\langle ij\rangle}-\frac{1}{2}J_{ij}(f^\dagger_{i\alpha}f_{j\alpha}f^\dagger_{j\beta}f_{j\beta}+\frac{1}{2}f^\dagger_{i\alpha}f_{i\alpha}f^\dagger_{j\beta}f_{j\beta})$. Because this representation enlarges the Hilbert space, states need to be constrained in the physical Hilbert space, i.e., one f-fermion per site:

$$f^\dagger_{i\alpha}f_{i\alpha}=1,\ f_{i\alpha}f_{i\beta}\epsilon_{\alpha\beta}=0. \tag{4}$$

Introducing mean-field parameters $\eta_{ij}\epsilon_{\alpha\beta}=-2\langle f_{i\alpha}f_{j\beta}\rangle$, $\chi_{ij}\delta_{\alpha\beta}=2\langle f^\dagger_{i\alpha}f_{j\beta}\rangle$, where $\epsilon_{\alpha\beta}$ is a fully antisymmetric tensor, after the Hubbard–Stratonovich transformation, the Lagrangian of the spin system can be written as[15]

$$L=\sum_i\psi^\dagger_i\partial_\tau\psi_i+\sum_{\langle ij\rangle}\frac{3}{8}J_{ij}\left[\frac{1}{2}\mathrm{Tr}\left(U^\dagger_{ij}U_{ij}\right)-(\psi^\dagger_iU_{ij}\psi_j+h.c.)\right]+\sum_i a^l_0(i)\psi^\dagger_i\tau^l\psi_i, \tag{5}$$

where two-component fermion notation $\psi_i=(f_{i,\uparrow},f^\dagger_{i,\downarrow})^T$ is introduced for reasons that will be explained shortly. U_{ij} is a matrix of mean-field amplitudes:

$$U_{ij}=\begin{pmatrix}\chi^\dagger_{ij} & \eta_{ij}\\ \eta^\dagger_{ij} & -\chi_{ij}\end{pmatrix}. \tag{6}$$

$a^l_0(i)$ are the local Lagrangian multipliers that enforce the constraints of Eq. (4).

In terms of ψ, Schwinger-fermion representation has an explicit SU(2) gauge redundancy: A transformation $\psi_i\to W_i\psi_i$, $U_{ij}\to W_iU_{ij}W^\dagger_j$, $W_i\in$ SU(2) leaves the action invariant. This redundancy originates from the representation of Eq. (3): This local SU(2) transformation leaves the spin operators invariant[18] and thus does not change physical Hilbert space.

One can try to solve Eq. (5) by a mean-field (or saddle-point) approximation. At the mean-field level, U_{ij} and a^l_0 are treated as complex numbers, and a^l_0 must be chosen such that constraints (4) are satisfied at the mean field level: $\langle\psi^\dagger_i\tau^l\psi_i\rangle=0$. The mean-field ansatz can be written as

$$H_{MF}=-\sum_{\langle ij\rangle}\psi^\dagger_iu_{ij}\psi_j+\sum_i\psi^\dagger_ia^l_0\tau^l\psi_i, \tag{7}$$

where $u_{ij}=\frac{3}{8}J_{ij}U_{ij}$. A local SU(2) gauge transformation modifies $u_{ij}\to W_iu_{ij}W^\dagger_j$ but does not change the physical spin state described by the mean-field ansatz. By construction, the mean-field amplitudes do not break spin-rotation symmetry,

and the mean-field solutions describe SL states if translational symmetry is preserved. Different $\{u_{ij}\}$ ansätze may be in different SL phases. The mathematical language to classify different SL phases is the PSG.[15]

The PSG is the manifestation of topological order in the Schwinger-fermion representation: SL states described by different PSG's are different phases. It is defined as the collection of all combinations of symmetry group and SU(2) gauge transformations that leave $\{u_{ij}\}$ invariant (as a_0^l are determined self-consistently by $\{u_{ij}\}$, these transformations also leave a_0^l invariant). The invariance of a mean-field ansatz $\{u_{ij}\}$ under an element of PSG $G_U U$ can be written as

$$\begin{gathered} G_U U(\{u_{ij}\}) = \{u_{ij}\}, \\ U(\{u_{ij}\}) \equiv \{\tilde{u}_{ij} = u_{U^{-1}(i),U^{-1}(j)}\}, \\ G_U(\{u_{ij}\}) \equiv \{\tilde{u}_{ij} = G_U(i) u_{ij} G_U(j)^\dagger\}, \\ G_U(i) \in \mathrm{SU}(2). \end{gathered} \tag{8}$$

Here $U \in SG$ is an element of the symmetry group (SG) of the SL state. The SG on a honeycomb lattice is generated by time reversal $\boldsymbol{T}$, reflection $\boldsymbol{\sigma}$, $\pi/3$ rotation C_6, and translations T_1, T_2, as illustrated in Fig. 1 (see also Appendix A). G_U is the gauge transformation associated with U such that $G_U U$ leaves $\{u_{ij}\}$ invariant.

There is an important subgroup of PSG, the invariant gauge group (IGG), which is composed of all the pure gauge transformations in PSG: IGG $\equiv \{\{W_i\} | W_i u_{ij} W_j^\dagger = u_{ij}, W_i \in \mathrm{SU}(2)\}$. One can always choose a gauge in which the elements in an IGG is site independent. In this gauge, IGG can be global Z_2 transformations $\{W_i = \tau^0, W_i = -\tau^0\}$; global $U(1)$ transformations $\{W_i = e^{i\theta\tau^3}, \theta \in [0, 2\pi]\}$; or global SU(2) transformations $\{W_i = e^{i\theta\hat{n}\cdot\vec{\tau}}, \theta \in [0, 2\pi], \hat{n} \in S^2\}$, and we dub them Z_2, $U(1)$, and SU(2) states, respectively.

The importance of the IGG is that it controls the low-energy gauge fluctuations. Beyond mean-field level, fluctuations of U_{ij} and a_0^l need to be considered and the mean-field state may or may not be stable. The low-energy effective theory is described by a fermionic spinon band structure coupled with a dynamical gauge field of an IGG. For example, the Z_2 state with gapped spinon dispersion can be a stable phase because the low-energy Z_2 dynamical gauge field can be in the deconfined phase.[36,37] But for a $U(1)$ state with gapped spinon dispersion, the $U(1)$ gauge fluctuations would generally drive the system into confinement due to monopole proliferation,[38] and the mean-field state would be unstable. And an SU(2) state with gapped spinon dispersion should also be in the confined phase because there is no known IR stable fixed point of pure SU(2) gauge theory in $2+1$ dimensions. Because the purpose of this paper is to search for SL liquid phases that have a Schwinger-fermion mean-field description, we will focus on Z_2 states.

If $G_U U \in$ PSG and $g \in$ IGG, by definition we have $g G_U U \in$ PSG. This means that the mapping h : PSG $\to$ SG : $f(G_U U) = U$ is a many-to-one mapping. In fact it is easy to show that mapping h induces group homomorphism[15]:

$$\mathrm{PSG}/\mathrm{IGG} = \mathrm{SG}. \tag{9}$$

Mathematically the PSG is an extension of the SG by the IGG.

Our definition of a PSG requires a mean-field ansatz $\{u_{ij}\}$. With Eq. (9), one can define an algebraic PSG which does not require ansatz $\{u_{ij}\}$. An algebraic PSG is simply defined as a group satisfying Eq. (9). Obviously a PSG (realizable by an ansatz) must be an algebraic PSG, but the reverse may not be true, because sometimes an algebraic PSG cannot be realized by any mean-field ansatz.

To classifying all possible Z_2 Schwinger-fermion mean-field states, we need to find all possible PSG extensions of the SG with a Z_2 IGG. Here SG is the direct product of the space group of the honeycomb lattice and the time-reversal Z_2 group. In Appendix A we show the general constraints that must be satisfied for such a group extension. In Appendix B, using these constraints, we find there are in total 160 Z_2 algebraic PSGs on a honeycomb lattice. And, at most, 128 PSGs of them can be realized by an ansatz $\{u_{ij}\}$. These 128 PSGs completely classify all Schwinger-fermion mean-field ansätze of Z_2 SLs on a honeycomb lattice.

III. Z_2 SPIN LIQUIDS ON A HONEYCOMB LATTICE AND THE SPS PHASE

Among the 128 states, can one further identify the candidate states for the SL discovered in the numerical study?[12] The answer is yes. Numerically the SL phase is found close to the Mott transition, and it seems to be connected to the semimetal phase by a continuous phase transition. What are the Z_2 Schwinger-fermion states in the neighborhood of the semimetal phase?

Are there Schwinger-fermion mean-field states that can be connected to the semimetal phase via a continuous phase transition? Physically a continuous Mott transition is associated with the loss of charge coherence of the electronic quasiparticles. The spinons in the Schwinger-fermion approach exactly describe these quasiparticles whose charge coherence has been lost.[22,23] The natural resulting SL phase is nothing but the state with a spinon band structure identical to the electronic one on the metallic side. In the present case this SL is the uniform RVB (u-RVB) state with a Dirac gapless spinon dispersion.[23] The nature of the Mott transtion between the semimetal phase and the u-RVB SL [referred to as the algebraic spin liquid (ASL) in Ref. 23] was studied by Hermele.[23] However, numerically it was shown that the SL phase is fully gapped. How to resolve this discrepancy?

This discrepancy is related to the stability issue of the ASL. The u-RVB (or ASL) ansatz can be simply expressed as a graphene-like nearest neighbor hopping of f-fermions:

$$H_{MF}^{\mathrm{uRVB}} = \chi \sum_{\langle ij \rangle} f_{i\alpha}^\dagger f_{j\alpha}, \tag{10}$$

where χ is real. The low energy effective theory of ASL is $2+1$D SU(2) QCD with $N_f = 2$ flavors of fermions,[23] i.e., QCD_3. In the large-N_f limit QCD_3 has a stable IR fixed point with gapless excitations and can be a stable ASL phase.[39] However the $N_f = 2$ case remains unclear. When $N_f = 0$ the pure gauge QCD_3 is in a confined phase.[40,41] This indicates a critical N_c, and, when $N_f < N_c$, confinement occurs.[39] Although no controlled estimate of N_c is available, a self-consistent solution of the Schwinger–Dyson equations[39]

suggests $N_c \approx \frac{64}{\pi^2}$, indicating that the $N_f = 2$ u-RVB (or ASL) state may not be a stable phase.

We find that the above-mentioned discrepancy can be resolved if we assume the ASL is not a stable phase but has one or more relavant couplings λ in the renormalization group sense. λ may be a four-fermion interaction. If λ is irrelevant at the Mott transition point (λ is dangerously irrelevant in this case), the Mott transition is still continuous and controlled by the fixed point studied in Ref. 23. We present the schematic RG flow in Fig. 2(b), and propose this scenario for the Mott transition in the simulated Hubbard model.

If this scenario is correct, the mean-field ansatz of the Z_2 SL should be connected to the u-RVB ansatz by a continuous Higgs condensation driven by the λ flow, which breaks the SU(2) IGG down to Z_2. During this transition, the u-RVB ansatz $\{u_{ij}^{\text{uRVB}}\} \to \{u_{ij}^{\text{uRVB}} + \delta u_{ij}\}$ and the δu_{ij} amplitudes play the role of the Higgs boson. We define a Z_2 state to be around (or in the neighborhood of) the u-RVB when the Z_2 state can be obtained by an infinitesimal change $\{u_{ij}^{\text{uRVB}}\} \to \{u_{ij}^{\text{uRVB}} + \delta u_{ij}\}$. Therefore this scenario dictate *the PSG of the Z_2 state to be a subgroup of the PSG of the ASL*. We propose this group-theoretical observation as a systematic way of identifying the SLs close to a continuous Mott transition: *The PSGs of these SLs are subgroups of the PSG of the "parent" SL whose spinon band structure is identical to the Fermi liquid.*

In Appendix C we classify all these possible PSG subgroups with the Z_2 IGG, which allows us to construct all possible Z_2 states around the u-RVB state. This technique was first developed by Wen.[15] We find that, among the 128 Z_2 states, there are a total 24 gauge-inequivalent Z_2 PSGs satisfying this condition, as listed in Table I in Appendix C.

TABLE I. A summary of all 24 different PSGs with IGG $= \{\pm\tau^0\}$ around the u-RVB ansatz. They correspond to 24 different Z_2 SLs near the u-RVB state.

No.	g_T	g_σ	g_{C_6}	g_1	g_2
1	τ^0	τ^0	τ^0	τ^0	τ^0
2	τ^0	τ^0	$i\tau^3$	τ^0	τ^0
3	τ^0	τ^0	$i\tau^3$	$e^{i2\pi/3\tau^1}$	$e^{-i2\pi/3\tau^1}$
4	τ^0	$i\tau^3$	$i\tau^3$	τ^0	τ^0
5	τ^0	$i\tau^3$	$i\tau^3$	τ^0	τ^0
6	τ^0	$i\tau^3$	$i\tau^1$	τ^0	τ^0
7	τ^0	$i\tau^3$	$e^{i\pi/6\tau^1}$	τ^0	τ^0
8	τ^0	$i\tau^3$	$e^{i\pi/3\tau^1}$	τ^0	τ^0
9	τ^0	$i\tau^3$	$i\tau^1$	$e^{i2\pi/3\tau^3}$	$e^{-i2\pi/3\tau^3}$
10	τ^0	$i\tau^3$	$e^{i2\pi/3\tau^1}$	$i\left(\frac{\tau^1}{\sqrt{3}} - \sqrt{\frac{2}{3}}\tau^2\right)$	$i\left(\frac{\tau^3}{\sqrt{2}} - \frac{\tau^2}{\sqrt{6}} - \frac{\tau^1}{\sqrt{3}}\right)$
11	$i\tau^3$	τ^0	τ^0	τ^0	τ^0
12	$i\tau^3$	τ^0	$i\tau^3$	τ^0	τ^0
13	$i\tau^3$	τ^0	$i\tau^1$	τ^0	τ^0
14	$i\tau^3$	τ^0	$i\tau^1$	$e^{i2\pi/3\tau^3}$	$e^{-i2\pi/3\tau^3}$
15	$i\tau^3$	$i\tau^3$	τ^0	τ^0	τ^0
16	$i\tau^3$	$i\tau^3$	$i\tau^3$	τ^0	τ^0
17	$i\tau^3$	$i\tau^3$	$i\tau^1$	τ^0	τ^0
18	$i\tau^3$	$i\tau^3$	$i\tau^1$	$e^{i2\pi/3\tau^3}$	$e^{-i2\pi/3\tau^3}$
19	$i\tau^3$	$i\tau^1$	$i\tau^1$	τ^0	τ^0
20	$i\tau^3$	$i\tau^1$	$i\tau^2$	τ^0	τ^0
21	$i\tau^3$	$i\tau^1$	τ^0	τ^0	τ^0
22	$i\tau^3$	$i\tau^1$	$i\tau^3$	τ^0	τ^0
23	$i\tau^3$	$i\tau^1$	$e^{i\pi/6\tau^3}$	τ^0	τ^0
24	$i\tau^3$	$i\tau^1$	$e^{i\pi/3\tau^3}$	τ^0	τ^0

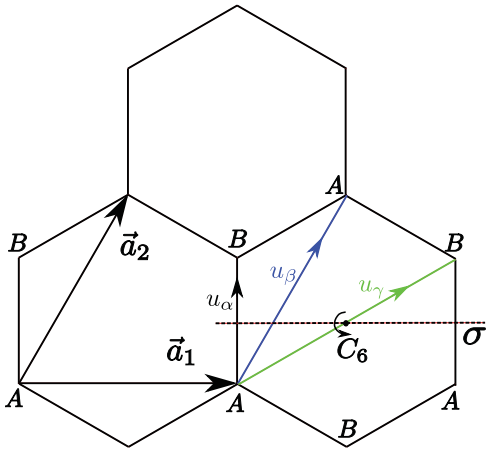

FIG. 3. (Color online) Honeycomb lattice and generators of symmetry group. u_α, u_β and u_γ are representatives of first, second, and third nearest-neighbor mean-field amplitudes.

Can these 24 Z_2 SL states have a full energy gap? We find that not all of them can have a gapped spinon spectrum. This can be understood starting from a Dirac dispersion of the u-RVB state. To gap out the Dirac nodes, at least one mass term in the low-energy effective theory of a given Z_2 state must be allowed by symmetry. In Appendix E we show that only 4 of the 24 Z_2 states allow a mass term in the low-energy theory. Thus only these 4 states are fully gapped Z_2 SLs around the u-RVB state. The other 20 states have symmetry-protected gapless spinon dispersions.

These four state are state numbers 16, 17, 19, and 22 in Table I in Appendix C. We can generate their mean-field ansätze by these PSGs. We find that up to the third neighbor mean-field amplitudes $u_{(\alpha,\beta,\gamma)}$, as shown in Fig. 3, only one of these four states can be realized, which is state 19. As shown in Appendix H, mean-field ansätze up to the third neighbor of the other three states actually have a $U(1)$ IGG. Only after introducing longer-range mean-field bonds can these three states have a Z_2 IGG. In particular, state 16 requires a fifth neighbor, state 17 requires fourth neighbor, and state 22 requires ninth neighbor amplitudes, while state 19 requires only second neighbor amplitudes. Because the t/U expansion of the Hubbard model give a rather short-range spin interaction for the SL phase found in numerics[12] ($t/U \sim 1/4$), the other three states are unlikely to be realized in a Hubbard model on a honeycomb lattice.

SPS is a fully gapped Z_2 SL on the honeycomb lattice. Its mean-field fermionic spinon band structure, after a proper gauge is choosen, is given as follows [Fig. 1(a)]:

$$H_{\text{SPS}}^{MF} = t_1 \sum_{\langle ij\rangle} f_{i\alpha}^\dagger f_{j\alpha} + t_2 \sum_{\langle\langle ij\rangle\rangle} f_{i\alpha}^\dagger f_{j\alpha} - \mu \sum_i f_{i\alpha}^\dagger f_{i\alpha} + \Delta \sum_{\langle\langle ij\rangle\rangle} \epsilon_{\alpha\beta} f_{i\alpha}^\dagger f_{j\beta}^\dagger + \text{h.c.} \quad (11)$$

where $t_{1,2}$ are real numbers. In the Schwinger-fermion approach, f-spinons are coupled to an SU(2) gauge field.[15,18]

However due to nonzero t_2 and Δ, the SU(2) gauge symmetry is reduced to Z_2 through the Higgs mechanism. Thus at low energy f-spinons are coupled to a dynamical Z_2 gauge field and stay in the deconfined phase. A Schwinger-fermion mean-field study of the J_1-J_2 Heisenberg model using the SPS ansatz is presented in Appendix F.

IV. CONTINUOUS PHASE TRANSITION FROM SPS TO CAF PHASE

We start from discussing the continuous phase transition from the SPS to the CAF phase in the Schwinger-fermion approach. How to describe an AF order in this approach? In Ref. 24, it is shown that the easy-plane AF order on a honeycomb lattice is described by a quantum spin Hall (QSH) band structure of spinons (spin quantized along the z axis) coupled with a dynamical $U(1)$ gauge field. The QSH effect binds the gauge fluctuation to the S^z spin density fluctuation, and the Goldstone mode of the easy-plane Néel order is nothing but photon of the $U(1)$ gauge field. A monopole quantum number[24] of the $U(1)$ gauge field shows the spin order is AF.

In the present spin-rotation symmetric system, we consider the phase described by a fluctuating $O(3)$ QSH order parameter $\vec{n}$, coupled with a $U(1)$ gauge field a_μ. Its mean-field ansatz is [Fig. 1(b)]

$$H^{MF}_{\mathrm{CAF}} = t_1 \sum_{\langle ij\rangle} f^\dagger_{i\alpha} f_{j\alpha} + t_2 \sum_{\langle\langle ij\rangle\rangle} f^\dagger_{i\alpha} f_{j\alpha} - \mu \sum_i f^\dagger_{i\alpha} f_{i\alpha} + \vec{n}\cdot \sum_{\langle\langle ij\rangle\rangle} i\nu_{ij} f^\dagger_{i\alpha} \vec{\sigma}_{\alpha\beta} f_{j\beta}. \quad (12)$$

There are three gapless modes in this phase: two $\hat{n}$ fluctuating modes and one photon mode. The photon mode is the in-plane spin wave of AF order $\vec{N}$ ($\vec{N} \perp \hat{n}$),[24] and the spin SU(2) symmetry is completely broken. Because $\hat{n}$ has the same symmetry as the QSH order, Eq. (12) is the representation of the CAF phase in the Schwinger-fermion method. The operation $C_6 \cdot \boldsymbol{T}$ [$\boldsymbol{T}$ is time reversal, C_6 is defined in Fig. 1(c)] leaves both order parameters invariant, indicating that the magnetic order in the CAF phase is still collinear.

Comparing Eq. (12) with Eq. (11), s-wave pairing Δ of spinons in the SPS phase is replaced by the $O(3)$ QSH order $\vec{n}$ in the CAF phase. If we group these orders together into a five-component vector $\vec{V} = (\mathrm{Re}\Delta, \mathrm{Im}\Delta, \vec{n})$, as pointed out in Ref. 25, fluctuations of $\vec{V}$ have a Wess–Zumino–Witten (WZW) Berry phase.[26] Physically it means that a skyrmion (antiskyrmion) of $\hat{n}$ in two spatial dimensions actually carries a fermion charge of 2 (-2). The hedgehog instanton of $\hat{n}$ in $2+1$ dimensions thus creates a charge-2 s-wave fermion pair. Therefore a continuous phase transition between a QSH insulator and an s-wave superconductor on the honeycomb lattice becomes possible.[25]

To discuss the CAF-SPS phase transition, it is convenient to introduce the CP^1 representation of the $\hat{n}$ order parameter: $\hat{n} = w^\dagger \vec{\sigma} w$, where $w = (w_1, w_2)^T$ are two complex numbers satisfying $|w_1|^2 + |w_2|^2 = 1$. This representation has a $U(1)$ gauge redundancy and thus w-bosons couple to a $U(1)$ gauge field A_μ. After integrating out the f-spinons (see Appendix G for details), we obtain the effective Lagrangian:

$$L = |(\partial_\mu - \mathrm{i}A_\mu)w|^2 + r|w|^2 + s|w|^4 + \frac{1}{2g_a^2} f_{\mu\nu}^2 + \frac{1}{2g_A^2} F_{\mu\nu}^2 + \frac{\mathrm{i}}{\pi}\epsilon_{\mu\nu\lambda} A_\mu \partial_\nu a_\lambda, \quad (13)$$

where $f_{\mu\nu} = \partial_\mu a_\nu - \partial_\nu a_\mu$ and $F_{\mu\nu} = \partial_\mu A_\nu - \partial_\nu A_\mu$ are gauge field strengths. [The constraint $|w_1|^2 + |w_2|^2 = 1$ can be enforced by a Lagrangian multiplier λ. Equation (13) can be obtained by the saddle point expansion of λ.] The last term, a mutual Chern–Simons (CS) term, is nothing but the WZW term in the gauge representation: It is well known that a skyrmion of $\hat{n}$ is a 2π A_μ gauge flux, which also carries two units of a_μ gauge charge due to the WZW term.

What are the phases described by the effective Lagrangian, Eq. (13)? When $r < 0$, the w-boson condenses and $\hat{n}$ is ordered, corresponding to the CAF phase. Here the mutual CS term does not qualitatively modify the low-energy dynamics due to the Higgs mechanism of A_μ. When $r > 0$, w-bosons are gapped and $\hat{n}$ is disordered; remarkably, Eq. (13) describes the Z_2 SPS phase. The identification of a $U(1)$ mutual CS theory and a Z_2 gauge theory has been studied before.[27,28] Here, with the WZW term, we are able to further identify the PSG of the Z_2 theory.

This identification is easily shown by studying the monopoles of a_μ and A_μ in Eq. (13). In $\hat{n}$ disordered phase, monopole events of both a_μ and A_μ are allowed. We denote their monopole creation operators as $V_a^\dagger$ and $V_A^\dagger$, respectively. The mutual CS term clearly dictates that an a_μ monopole creates two units of A_μ gauge charge, and vice versa. These events mean that $f_\alpha^\dagger f_\beta^\dagger$ and $w_\alpha^\dagger w_\beta^\dagger$ pairing terms exist, which break the $U(1)$ gauge group down to Z_2. The WZW term indicates that the f-spinon pairing is s-wave, and thus the system is in SPS phase.

The mutual CS term also dictates that the f-spinon and w-boson satisfy mutual semion statistics. Namely they see each other as a π flux and are dual degrees of freedom. We can focus on either set of dual variables, $f(V_A^\dagger)$ or $w(V_a^\dagger)$, to write the effective theory. Because the phase transition from the SPS to CAF phase is described by w-boson condensation in Eq. (13), we will use $w(V_a^\dagger)$ variables in the next section.

V. DUALITY BETWEEN SCHWINGER-FERMION AND SCHWINGER-BOSON REPRESENTATIONS

In this section we focus on the dual variables of f-spinons: the w-bosons. The SPS phase is then a Z_2 phase with w-bosons as Z_2 charges, but f-spinons as visons. In this formulation SPS-CAF phase transition is naturally presented as a Higgs condensation of w-bosons.

First we need to represent the order parameters of the CAF phase in terms of w. The QSH order is $\hat{n} = w^\dagger \vec{\sigma} w$, but what is the Néel order parameter? Néel order in CAF phase corresponds to the monopole of a_μ, namely a pairing of w-bosons. There are two spin-1 bosonic pairing order parameters

satisfying this requirement, i.e., the real and imaginary parts of $(i\sigma_y w^*)^\dagger \vec{\sigma} w$:

$$\hat{n}_1 + i\hat{n}_2 = (i\sigma_y w^*)^\dagger_\alpha \vec{\sigma}_{\alpha\beta} w_\beta. \tag{14}$$

It is easy to verify that $\hat{n} = \hat{n}_1 \times \hat{n}_2$, so there are only two independent vectorial order parameters. The issue is, which one is the Néel order parameter $\vec{N}$: $\hat{n}_1$ or $\hat{n}_2$?

A $U(1)$ gauge transformation $w \to e^{i\theta} w$ generates a rotation in the $\hat{n}_1$,$\hat{n}_2$ plane. By fixing a proper gauge, we can always choose $\hat{n}_1$ as the Néel order. We will work within this gauge $\vec{N} = \hat{n}_1$ throughout the phase transition. Such a gauge fixing breaks the $U(1)$ gauge redundancy down to Z_2: $w \to \pm w$.

The physical symmetries of the QSH (or vector spin chirality) and the Néel order parameters completely determine the transformation rules of the w-boson up to a Z_2 gauge redundancy:

$$\begin{array}{rlll} T_1,T_2: & \hat{n} \to \hat{n}, & \vec{N} \to \vec{N}, & w \to w, \\ \boldsymbol{T}: & \hat{n} \to \hat{n}, & \vec{N} \to -\vec{N}, & w \to i w^*, \\ \sigma: & \hat{n} \to -\hat{n}, & \vec{N} \to -\vec{N}, & w \to i\sigma_y w^*, \\ C_6: & \hat{n} \to \hat{n}, & \vec{N} \to -\vec{N}, & w \to i w, \end{array} \tag{15}$$

where time-reversal transformation $\boldsymbol{T}$ is anti-unitary. The reason why there is no further arbitrariness on the transformation rules of w can be easily understood by the following construction. If we write w-boson as an $SU(2)$ matrix,

$$U = \begin{pmatrix} w_1 & w_2^* \\ w_2 & -w_1^* \end{pmatrix}, \tag{16}$$

then the most general $O(4)$ transformation leaving $|w_1|^2 + |w_2|^2 = 1$ is $U \to V_L U V_R$, where V_L and V_R are both SU(2) rotations (V_L is spin rotation) and $O(4) \sim \mathrm{SU}(2)_L \times \mathrm{SU}(2)_R$. In this representation, the vectors $\hat{n}_1$,$\hat{n}_2$,$\hat{n}$ are the first, second and third columns of a 3×3 rotation matrix R:[49]

$$R^{ab} = \tfrac{1}{2}\mathrm{Tr}(U^\dagger \sigma^a U \sigma^b). \tag{17}$$

Clearly, to leave R invariant, the transformations $V_{L,R}$ must be ± 1.

These symmetry transformation rules allow us to reveal the connection between the SPS state here and the zero-flux state in the Schwinger-boson representation obtained by Wang.[13] In Wang's work, the Néel order is represented by the z-boson as $\vec{N} = z^\dagger \vec{\sigma} z$ in the effective theory. From Eq. (17), we can easily construct the duality transformation between the w-boson and z-boson representations: $U_w = U_z V_R$, $V_R = e^{i\frac{\pi}{4}\sigma_y}$, namely,

$$w = \tfrac{1}{\sqrt{2}}(z - i\sigma^y z^*) \quad \text{or} \quad z = \frac{1}{\sqrt{2}}(w + i\sigma^y w^*). \tag{18}$$

Under duality transformation,

$$\begin{aligned} \vec{N} &= \mathrm{Re}[(i\sigma_y w^*)^\dagger \vec{\sigma} w] = z^\dagger \vec{\sigma} z, \\ \hat{n} &= w^\dagger \vec{\sigma} w = -\mathrm{Re}[(i\sigma_y z^*)^\dagger \vec{\sigma} z]. \end{aligned} \tag{19}$$

From Eq. (15) and (18), we can obtain transformation rules of z-bosons:

$$\begin{array}{rl} T_1,T_2: & z \to z, \\ \boldsymbol{T}: & z \to \sigma_y z, \\ \sigma: & z \to i\sigma_y z^*, \\ C_6: & z \to \sigma_y z^*, \end{array} \tag{20}$$

which are exactly the transformation rules found by Wang[13] for the zero-flux state up to a Z_2 gauge arbitrariness. This explicitly confirms that the z-bosons constructed in Eq. (18) are the same z-bosons discussed by Wang, and the SPS phase here is identical to the zero-flux phase in Schwinger-boson description.

Following the discussion in Ref. 2, we can write down the general symmetry-allowed effective theory for the phase transition in terms of the z-boson:

$$\begin{aligned} L = {} & |\partial_\tau z|^2 + c^2 |\nabla z|^2 + m^2 |z|^2 + u(|z|^2)^2 \\ & + \lambda_H \, (i\sigma_y z^*)^\dagger \left[\sum_i (\vec{d}_i \cdot \nabla)^3 \right] z + \text{h.c.} \end{aligned} \tag{21}$$

Here λ_H is the Higgs coupling which reduces the gauge degrees of freedom in the z-boson formulation down to Z_2. $\vec{d}_1 = -\vec{a}_1$, $\vec{d}_2 = \vec{a}_2$, and $\vec{d}_3 = \vec{a}_1 - \vec{a}_2$, as shown in Fig. 1. For instance, the single time derivative term $z^\dagger \partial_\tau z$ is forbidden by σ, and $z^T(-i\sigma_y)\partial_\tau z$ is forbidden by C_6. The Higgs coupling can also be written as a pairing of w-bosons: $\lambda_H \, (i\sigma_y w^*)^\dagger [\sum_i (\vec{d}_i \cdot \nabla)^3] w + \text{h.c.}$ By naive power counting, λ_H is irrelevant; therefore we have an $O(4)$ critical point between the CAF (z-condensed) phase and the SPS (z-gapped) phase. The critical behavior of this transition is well-studied.[29–31]

VI. SUMMARY

In this paper, our main prediction is the CAF phase. Unlike, the usual AF (Néel) phase, the CAF phase has two order parameters: Néel order $\vec{N}$ and QSH order $\hat{n}$. As the CAF phase is likely to be the magnetically ordered phase adjacent to the SL phase found in the numeric study,[12] in the following we propose explicit numerical methods to detect the CAF phase.

One can directly measure QSH order by $\langle \vec{n}(x) \cdot \vec{n}(0) \rangle$ correlation function, or the spin vector-chirality correlation $\langle (\nu_{i+x,j+x} \vec{S}_{i+x} \times \vec{S}_{j+x}) \cdot (\nu_{ij} \vec{S}_i \times \vec{S}_j) \rangle$. Since the QSH order is odd under $\sigma \cdot \boldsymbol{T}$ while the Néel order is $\sigma \cdot \boldsymbol{T}$-even, one does not expect a long-range correlation of QSH order in a usual Néel phase. Therefore, the long range QSH correlation is an intrinsic signature of the CAF phase. In addition, one can check that the QSH vector is normal to the Néel vector. For example, one can pin the Néel order by an infinitesimal (in thermodynamic limit) staggered magnetic field along the z axis, and the measured QSH order parameters should only have x,y components. Experimentally such an exotic SL may be realized in candidate systems such as expanded graphene-like system in group IV elements[32,33] and fermions in optical lattices.[34,35]

ACKNOWLEDGMENTS

YR thanks Ashvin Vishwanath for helpful comments. YML acknowledges support from DOE under Grant No. DE-FG02-99ER45747. YR is supported by the startup fund at Boston College.

APPENDIX A: GENERAL CONDITIONS ON PROJECTIVE SYMMETRY GROUP OF SYMMETRIC SPIN LIQUIDS ON A HONEYCOMB LATTICE

As mentioned in Section II, the SG on a honeycomb lattice is generated by time-reversal transformation $\boldsymbol{T}$, translations along $\vec{a}_1,\vec{a}_2$: T_1,T_2, plaquette-centered 60° C_6 rotation, and a horizontal mirror reflection $\boldsymbol{\sigma}$, as shown in Fig. 1. In the present problem, the symmetry group SG can be represented as

$$\mathrm{SG} = \left\{U = \boldsymbol{T}^{\nu_T}\cdot T_1^{\nu_{T_1}}\cdot T_2^{\nu_{T_2}}\cdot C_6^{\nu_{C_6}}\cdot\boldsymbol{\sigma}^{\nu_\sigma}\right\},$$

where $\nu_{T_1},\nu_{T_2}\in\boldsymbol{Z}$ and $\nu_{\boldsymbol{T}},\nu_{\boldsymbol{\sigma}}\in\boldsymbol{Z}_2$, $\nu_{C_6}\in\boldsymbol{Z}_6$, since the generators satisfy

$$\boldsymbol{T}^2=\boldsymbol{\sigma}^2=(C_6)^6=1. \tag{A1}$$

Here 1 stands for the identity element of the SG. To completely determine the multiplication rule of this group, we need to identify the multiplication rule of two different generators in an order different from $\boldsymbol{T}^{\nu_T}\cdot T_1^{\nu_{T_1}}\cdot T_2^{\nu_{T_2}}\cdot C_6^{\nu_{C_6}}\cdot\boldsymbol{\sigma}^{\nu_\sigma}$:

$$\begin{aligned}
U\boldsymbol{T} &= \boldsymbol{T}U(U=T_1,T_2,C_6,\boldsymbol{\sigma}), && \text{(A2)}\\
T_1T_2 &= T_2T_1, && \text{(A3)}\\
C_6T_1 &= T_2C_6, && \text{(A4)}\\
C_6T_2 &= T_1^{-1}T_2C_6, && \text{(A5)}\\
\boldsymbol{\sigma}T_1 &= T_1\boldsymbol{\sigma}, && \text{(A6)}\\
\boldsymbol{\sigma}T_2 &= T_1T_2^{-1}\boldsymbol{\sigma}, && \text{(A7)}\\
\boldsymbol{\sigma}C_6 &= C_6^{-1}\boldsymbol{\sigma}, && \text{(A8)}
\end{aligned}$$

The above relations can be written in an alternative way:

$$\begin{aligned}
\boldsymbol{T}^2=\boldsymbol{\sigma}^2=(C_6)^6&=1, && \text{(A9)}\\
\boldsymbol{T}U\boldsymbol{T}^{-1}U^{-1}&=1(U=T_1,T_2,C_6,\boldsymbol{\sigma}), && \text{(A10)}\\
T_1T_2T_1^{-1}T_2^{-1}&=1, && \text{(A11)}\\
T_2^{-1}C_6T_1C_6^{-1}&=1, && \text{(A12)}\\
T_1^{-1}C_6T_1T_2^{-1}C_6^{-1}&=1, && \text{(A13)}\\
T_1^{-1}\boldsymbol{\sigma}T_1\boldsymbol{\sigma}^{-1}&=1, && \text{(A14)}\\
T_2^{-1}\boldsymbol{\sigma}T_1T_2^{-1}\boldsymbol{\sigma}^{-1}&=1, && \text{(A15)}\\
\boldsymbol{\sigma}C_6\boldsymbol{\sigma}C_6&=1, && \text{(A16)}
\end{aligned}$$

which determine the inverses of all the group elements.

As introduced in Section II, the mean-field ansatz $\{u_{ij}\}$ of a SL is invariant under the action of any element G_UU of a projective symmetry group (PSG). The multiplication rule of the SG would immediately enforce the following constraints on a PSG by its definition: if $U_1U_2=U_3$ then

$$\begin{aligned}
&G_{U_1}U_1G_{U_2}U_2(\{u_{ij}\}) = G_{U_3}U_3(\{u_{ij}\})\\
\Longrightarrow&\left[G_{U_1}(U_1U_2(i))G_{U_2}(U_2(i))\right]u_{ij}\left[G_{U_1}(U_1U_2(i))G_{U_2}(U_2(i))\right]^\dagger\\
&\quad=[G_{U3}(U_3(i))]u_{ij}[G_{U3}(U_3(i))]^\dagger,\ \forall i,j. \qquad \text{(A17)}
\end{aligned}$$

On the other hand, we know that those pure gauge transformations, under which the mean-field ansatz $\{u_{ij}\}$ is invariant, constitute a subgroup of PSG, coined the invariant gauge group (IGG):

$$\mathrm{IGG}=\{W_i|W_iu_{ij}W_j^\dagger=u_{ij},W_i\in\mathrm{SU}(2)\}. \tag{A18}$$

Therefore from Eq. (A17) we have the following constraints on the elements of a PSG

$$\left[G_{U_1U_2}(U_1U_2(i))\right]^\dagger G_{U_1}(U_1U_2(i))G_{U_2}(U_2(i))=\mathcal{G}\in\mathrm{IGG}.$$

The above condition holds for any two group elements U_1,U_2 of a SG. Similar with a SG, we can choose a set of generators in any given a PSG: $\{G_{T_1}T_1,G_{T_2}T_2,G_{\boldsymbol{T}}\boldsymbol{T},G_{C_6}C_6,G_{\boldsymbol{\sigma}}\boldsymbol{\sigma}\}$. Any given element in a PSG can be written in the standard form:

$$\begin{aligned}
G_UU=&(G_{\boldsymbol{T}}\boldsymbol{T})^{\nu_T}\cdot\left(G_{T_1}T_1\right)^{\nu_{T_1}}\cdot\left(G_{T_2}T_2\right)^{\nu_{T_2}}\\
&\cdot\left(G_{C_6}C_6\right)^{\nu_{C_6}}\cdot(G_{\boldsymbol{\sigma}}\boldsymbol{\sigma})^{\nu_\sigma}. \qquad \text{(A19)}
\end{aligned}$$

Since the multiplication rule of a SG on a honeycomb lattice is completely determined by Eqs. (A1)–(A8), or equivalently Eqs. (A9)–(A16), the only independent constraints on the PSG generators are the following:

$$\begin{aligned}
&(G_{\boldsymbol{T}}\boldsymbol{T})^2\in\mathrm{IGG},(G_{\boldsymbol{\sigma}}\boldsymbol{\sigma})^2\in\mathrm{IGG},\\
&\left(G_{C_6}C_6\right)^6\in\mathrm{IGG},\\
&\left(G_{T_1}T_1\right)^{-1}\left(G_{T_2}T_2\right)^{-1}\left(G_{T_1}T_1\right)\left(G_{T_2}T_2\right)\in\mathrm{IGG},\\
&\left(G_{T_1}T_1\right)^{-1}(G_{\boldsymbol{T}}\boldsymbol{T})^{-1}\left(G_{T_1}T_1\right)(G_{\boldsymbol{T}}\boldsymbol{T})\in\mathrm{IGG},\\
&\left(G_{T_2}T_2\right)^{-1}(G_{\boldsymbol{T}}\boldsymbol{T})^{-1}\left(G_{T_2}T_2\right)(G_{\boldsymbol{T}}\boldsymbol{T})\in\mathrm{IGG},\\
&\left(G_{T_2}T_2\right)^{-1}\left(G_{C_6}C_6\right)\left(G_{T_1}T_1\right)\left(G_{C_6}C_6\right)^{-1}\in\mathrm{IGG},\\
&\left(G_{T_1}T_1\right)^{-1}\left(G_{C_6}C_6\right)\left(G_{T_1}T_1\right)\left(G_{T_2}T_2\right)^{-1}\left(G_{C_6}C_6\right)^{-1}\in\mathrm{IGG},\\
&(G_{\boldsymbol{T}}\boldsymbol{T})^{-1}\left(G_{C_6}C_6\right)^{-1}(G_{\boldsymbol{T}}\boldsymbol{T})\left(G_{C_6}C_6\right)\in\mathrm{IGG}, \qquad \text{(A20)}\\
&\left(G_{T_1}T_1\right)^{-1}(G_{\boldsymbol{\sigma}}\boldsymbol{\sigma})\left(G_{T_1}T_1\right)(G_{\boldsymbol{\sigma}}\boldsymbol{\sigma})^{-1}\in\mathrm{IGG},\\
&\left(G_{T_2}T_2\right)^{-1}(G_{\boldsymbol{\sigma}}\boldsymbol{\sigma})\left(G_{T_1}T_1\right)\left(G_{T_2}T_2\right)^{-1}(G_{\boldsymbol{\sigma}}\boldsymbol{\sigma})^{-1}\in\mathrm{IGG},\\
&(G_{\boldsymbol{\sigma}}\boldsymbol{\sigma})\left(G_{C_6}C_6\right)(G_{\boldsymbol{\sigma}}\boldsymbol{\sigma})\left(G_{C_6}C_6\right)\in\mathrm{IGG},\\
&(G_{\boldsymbol{T}}\boldsymbol{T})^{-1}(G_{\boldsymbol{\sigma}}\boldsymbol{\sigma})^{-1}(G_{\boldsymbol{T}}\boldsymbol{T})(G_{\boldsymbol{\sigma}}\boldsymbol{\sigma})\in\mathrm{IGG},
\end{aligned}$$

or more specifically

$$\begin{aligned}
&[G_{\boldsymbol{T}}(i)]^2\in\mathrm{IGG},\\
&G_{\boldsymbol{\sigma}}(\boldsymbol{\sigma}(i))G_{\boldsymbol{\sigma}}(i)\in\mathrm{IGG},\\
&G_{C_6}\left(C_6^{-1}(i)\right)G_{C_6}\left(C_6^{-2}(i)\right)G_{C_6}\left(C_6^3(i)\right)\\
&\cdot G_{C_6}\left(C_6^2(i)\right)G_{C_6}(C_6(i))G_{C_6}(i)\in\mathrm{IGG},\\
&G_{T_1}^{-1}\left(T_2^{-1}T_1(i)\right)G_{T_2}^{-1}(T_1(i))G_{T_1}(T_1(i))G_{T_2}(i)\in\mathrm{IGG},\\
&G_{T_1}^{-1}(T_1(i))G_{\boldsymbol{T}}^{-1}(T_1(i))G_{T_1}(T_1(i))G_{\boldsymbol{T}}(i)\in\mathrm{IGG},\\
&G_{T_2}^{-1}(T_2(i))G_{\boldsymbol{T}}^{-1}(T_2(i))G_{T_2}(T_2(i))G_{\boldsymbol{T}}(i)\in\mathrm{IGG},\\
&G_{T_2}^{-1}(T_2(i))G_{C_6}(T_2(i))G_{T_1}\left(T_1C_6^{-1}(i)\right)G_{C_6}^{-1}(i)\in\mathrm{IGG},\\
&G_{T_1}^{-1}(T_1(i))G_{C_6}(T_1(i))G_{T_1}\left(C_6^{-1}T_1(i)\right) \qquad \text{(A21)}\\
&\cdot G_{T_2}^{-1}\left(C_6^{-1}(i)\right)G_{C_6}^{-1}(i)\in\mathrm{IGG},\\
&G_{\boldsymbol{T}}^{-1}\left(C_6^{-1}(i)\right)G_{C_6}^{-1}(i)G_{\boldsymbol{T}}(i)G_{C_6}(i)\in\mathrm{IGG},\\
&G_{T_1}^{-1}(T_1(i))G_{\boldsymbol{\sigma}}(T_1(i))G_{T_1}(T_1\boldsymbol{\sigma}^{-1}(i))G_{\boldsymbol{\sigma}}^{-1}(i)\in\mathrm{IGG},\\
&G_{T_2}^{-1}(T_2(i))G_{\boldsymbol{\sigma}}(T_2(i))G_{T_1}(\boldsymbol{\sigma}T_2(i))G_{T_2}^{-1}(\boldsymbol{\sigma}(i))G_{\boldsymbol{\sigma}}^{-1}(i)\in\mathrm{IGG},\\
&G_{\boldsymbol{\sigma}}(i)G_{C_6}(\boldsymbol{\sigma}(i))G_{\boldsymbol{\sigma}}(\boldsymbol{\sigma}C_6(i))G_{C_6}(C_6(i))\in\mathrm{IGG},\\
&G_{\boldsymbol{T}}^{-1}(\boldsymbol{\sigma}(i))G_{\boldsymbol{\sigma}}^{-1}(i)G_{\boldsymbol{T}}(i)G_{\boldsymbol{\sigma}}(i)\in\mathrm{IGG}.
\end{aligned}$$

The preceding relations are all the general consistent conditions to be satisfied by the generators of a PSG on a honeycomb lattice.

We will use (x_1,x_2,s) to label a site i in a honeycomb lattice, where x_1,x_2 are the coordinates of the unit cell in basis $\vec{a}_1,\vec{a}_2$ and $s=0,1$ for A and B sublattices respectively. For convenience, we summarize the coordinate transformations of all the generators in the SG group on a honeycomb lattice as follows:

$$\begin{aligned}
\boldsymbol{T} &: (x_1,x_2,s) \to (x_1,x_2,s),\\
T_1 &: (x_1,x_2,s) \to (x_1+1,x_2,s),\\
T_2 &: (x_1,x_2,s) \to (x_1,x_2+1,s),\\
\boldsymbol{\sigma} &: (x_1,x_2,s) \to (x_1+x_2,-x_2,1-s),\\
C_6 &: (x_1,x_2,0) \to (1-x_2,x_1+y_1-1,1)\\
&\quad (x_1,x_2,1) \to (-x_2,x_1+y_1,0).
\end{aligned} \tag{A22}$$

APPENDIX B: CLASSIFICATION OF Z_2 PROJECTIVE SYMMETRY GROUPS ON A HONEYCOMB LATTICE

As discussed in Section II, the problem of classifying all possible Z_2 Schwinger-fermion mean-field states is mathematically reduced to finding all possible PSGs. Let us firstly find all algebraic PSGs.

1. General discussion

In the case of Z_2 spin liquids, the IGG of the corresponding PSG is a Z_2 group: IGG $=\{\pm\tau^0\}$. The constraints listed in Appendix A now become

$$[G_{\boldsymbol{T}}(i)]^2=\eta_{\boldsymbol{T}}\tau^0, \tag{B1}$$

$$G_{\boldsymbol{\sigma}}(\boldsymbol{\sigma}(i))G_{\boldsymbol{\sigma}}(i)=\eta_{\boldsymbol{\sigma}}\tau^0, \tag{B2}$$

$$G_{C_6}\big(C_6^{-1}(i)\big)G_{C_6}\big(C_6^{-2}(i)\big)G_{C_6}\big(C_6^{3}(i)\big) \tag{B3}$$

$$\cdot\, G_{C_6}\big(C_6^{2}(i)\big)G_{C_6}(C_6(i))G_{C_6}(i)=\eta_{C_6}\tau^0, \tag{B4}$$

$$G_{T_1}^{-1}\big(T_2^{-1}T_1(i)\big)G_{T_2}^{-1}(T_1(i)) \cdot G_{T_1}(T_1(i))G_{T_2}(i)=\eta_{12}\tau^0, \tag{B5}$$

$$G_{T_1}^{-1}(T_1(i))G_{\boldsymbol{T}}^{-1}(T_1(i))G_{T_1}(T_1(i))G_{\boldsymbol{T}}(i)=\eta_{1\boldsymbol{T}}\tau^0, \tag{B6}$$

$$G_{T_2}^{-1}(T_2(i))G_{\boldsymbol{T}}^{-1}(T_2(i))G_{T_2}(T_2(i))G_{\boldsymbol{T}}(i)=\eta_{2\boldsymbol{T}}\tau^0, \tag{B7}$$

$$G_{T_2}^{-1}(T_2(i))G_{C_6}(T_2(i)) \cdot G_{T_1}\big(T_1C_6^{-1}(i)\big)G_{C_6}^{-1}(i)=\eta_{C_61}\tau^0, \tag{B8}$$

$$G_{T_1}^{-1}(T_1(i))G_{C_6}(T_1(i))G_{T_1}\big(C_6^{-1}T_1(i)\big) \cdot G_{T_2}^{-1}\big(C_6^{-1}(i)\big)G_{C_6}^{-1}(i)=\eta_{C_62}\tau^0, \tag{B9}$$

$$G_{\boldsymbol{T}}^{-1}\big(C_6^{-1}(i)\big)G_{C_6}^{-1}(i)G_{\boldsymbol{T}}(i)G_{C_6}(i)=\eta_{C_6\boldsymbol{T}}\tau^0, \tag{B10}$$

$$G_{T_1}^{-1}(T_1(i))G_{\boldsymbol{\sigma}}(T_1(i)) \cdot G_{T_1}\big(T_1\boldsymbol{\sigma}^{-1}(i)\big)G_{\boldsymbol{\sigma}}^{-1}(i)=\eta_{\sigma 1}\tau^0, \tag{B11}$$

$$G_{T_2}^{-1}(T_2(i))G_{\boldsymbol{\sigma}}(T_2(i))G_{T_1}(\boldsymbol{\sigma}T_2(i)) \cdot G_{T_2}^{-1}(\boldsymbol{\sigma}(i))G_{\boldsymbol{\sigma}}^{-1}(i)=\eta_{\sigma 2}\tau^0, \tag{B12}$$

$$G_{\boldsymbol{\sigma}}(i)G_{C_6}(\boldsymbol{\sigma}(i)) \cdot G_{\boldsymbol{\sigma}}(\boldsymbol{\sigma}C_6(i))G_{C_6}(C_6(i))=\eta_{\sigma C_6}\tau^0, \tag{B13}$$

$$G_{\boldsymbol{T}}^{-1}(\boldsymbol{\sigma}(i))G_{\boldsymbol{\sigma}}^{-1}(i)G_{\boldsymbol{T}}(i)G_{\boldsymbol{\sigma}}(i)=\eta_{\sigma\boldsymbol{T}}\tau^0, \tag{B14}$$

where all the η's take values of ±1. Not all of these conditions are gauge independent. Because we can rechoose the gauge part of generators such as $G_{T_1},G_{T_2}\ldots$ by multiplying them by $-\tau^0$ (an element of the IGG), only those conditions in which the same generator shows up twice are gauge independent. We can use this gauge dependence to simplify these conditions. Because $G_{T_1}(G_{T_2})$ only shows up once in the equation of $\eta_{C_61}(\eta_{C_62})$, we can always choose a gauge such that $\eta_{C_61}=\eta_{C_62}=1$. All other η's are gauge independent.

In the following we will determine all the possible PSG's with different (gauge-inequivalent) elements $\{G_U(i)\}$. These different PSG's characterize all the different type of Z_2 SLs on a honeycomb lattice, which might be constructed from a mean-field ansatz $\{u_{ij}\}$.

First notice that under a local SU(2) gauge transformation $u_{ij}\to W_iu_{ij}W_j^\dagger$, the PSG elements transform as $G_U(i)\to W_iG_U(i)W_{U^{-1}(i)}^\dagger$. Making use of such a degree of freedom, we can always choose proper gauge so that

$$G_{T_1}(x_1,x_2,s)=G_{T_2}(0,x_2,s)=\tau^0, x_1,x_2\in\mathbb{Z}.$$

Now taking Eq. (B5) into account, we have $G_{T_2}(\{x_1+1,x_2,s\})=\eta_{12}G_{T_2}(\{x_1,x_2,s\})$ and therefore

$$G_{T_1}(x_1,x_2,s)=\tau^0,\quad G_{T_2}(x_1,x_2,s)=\eta_{12}^{x_1}\tau^0. \tag{B15}$$

Meanwhile, from Eqs. (B1), (B6), and (B7) we can immediately see that $\eta_{1\boldsymbol{T}}=\eta_{2\boldsymbol{T}}=1$, and the gauge-inequivalent choices of $G_{\boldsymbol{T}}(i)$ are the following:

$$G_{\boldsymbol{T}}(x_1,x_2,s)=g_{\boldsymbol{T}}(s)=\begin{cases}\eta_t^s\tau^0, & \eta_{\boldsymbol{T}}=1\\ i\tau^3, & \eta_{\boldsymbol{T}}=-1\end{cases}, \tag{B16}$$

where $\eta_t=\pm1$.

As discussed earlier, we can always choose a proper gauge so that $\eta_{C_61}=\eta_{C_62}=1$. Then conditions (B8) and (B9) we see that

$$G_{C_6}(x_1,x_2,s)=\eta_{12}^{x_1x_2+x_1(x_1-1)/2}g_{C_6}(s); \tag{B17}$$

similarly from conditions (B11) and (B12) we have

$$G_{\boldsymbol{\sigma}}(x_1,x_2,s)=\eta_{\boldsymbol{\sigma}1}^{x_1}\eta_{\boldsymbol{\sigma}2}^{x_2}\eta_{12}^{x_2(x_2-1)/2}g_{\boldsymbol{\sigma}}(s), \tag{B18}$$

where $g_{C_6}(s),g_{\boldsymbol{\sigma}}(s)\in$ SU(2). Note that Eqs. (B2) and (B13) give further constraints to expression (B18):

$$\eta_{\boldsymbol{\sigma}1}=\eta_{\boldsymbol{\sigma}2}=\eta_{12}. \tag{B19}$$

Now we see that the elements of the PSG can be expressed as

$$G_{T_1}(x_1,x_2,s)=\tau^0, \tag{B20}$$

$$\begin{aligned}
G_{T_2}(x_1,x_2,s)&=\eta_{12}^{x_1}\tau^0,\\
G_{\boldsymbol{T}}(x_1,x_2,s)&=g_{\boldsymbol{T}}(s),\\
G_{C_6}(x_1,x_2,s)&=\eta_{12}^{x_1x_2+x_1(x_1-1)/2}g_{C_6}(s),\\
G_{\boldsymbol{\sigma}}(x_1,x_2,s)&=\eta_{12}^{x_1+x_2(x_2+1)/2}g_{\boldsymbol{\sigma}}(s).
\end{aligned} \tag{B21}$$

Consistent conditions (B2), (B4), (B10), (B13), and (B14) correspond to the following constraints on SU(2) matrices

$g_{C_6}(s), g_{\boldsymbol{\sigma}}(s)$:

$$\begin{aligned} g_{\boldsymbol{\sigma}}(0)g_{\boldsymbol{\sigma}}(1) &= \eta_{\boldsymbol{\sigma}}\tau^0, \\ [g_{C_6}(s)g_{C_6}(1-s)]^3 &= \eta_{C_6}\eta_{12}\tau^0, \\ g_{\boldsymbol{T}}(s)g_{C_6}(s) &= g_{C_6}(s)g_{\boldsymbol{T}}(1-s)\eta_{C_6\boldsymbol{T}}, \\ g_{\boldsymbol{T}}(s)g_{\boldsymbol{\sigma}}(s) &= g_{\boldsymbol{\sigma}}(s)g_{\boldsymbol{T}}(1-s)\eta_{\boldsymbol{\sigma}\boldsymbol{T}}, \\ g_{\boldsymbol{\sigma}}(s)g_{C_6}(1-s) &= \begin{cases} \lambda^s_{C_6}\tau^0, & \eta_{\boldsymbol{\sigma}C_6}=1 \\ \mathrm{i}\hat{n}_s\cdot\vec{\tau}, & \eta_{\boldsymbol{\sigma}C_6}=-1 \end{cases}, \end{aligned} \tag{B22}$$

where $\lambda_{C_6} = \pm 1$ and $\hat{n}_s$ is a unit vector.

2. A summary of 160 different PSGs

Below we summarize the 160 possible PSGs obtained through solving (B22). We use capital Roman numerals (I) and (II) to label $g_{\boldsymbol{T}} = \eta^s_t\tau^0$ and $g_{\boldsymbol{T}} = i\tau^3$, respectively. Roman numerals (i) and (ii) are used to label $\eta_{C_6\boldsymbol{T}} = \pm 1$, respectively. (A) and (B) are used to label $\eta_{\boldsymbol{\sigma}C_6} = \pm 1$, respectively. Finally, (α) and (β) are used to label $\eta_{\boldsymbol{\sigma}\boldsymbol{T}}$, respectively.

(I) $g_{\boldsymbol{\sigma}T} = \eta^s_t\tau^0$.

It is easy to see that $\eta_{C_6\boldsymbol{T}} = \eta_{\boldsymbol{\sigma}\boldsymbol{T}} = \eta_t$ from Eq. (B22), so there is the only possibility among (i) and (ii).

(A) $g_{\boldsymbol{\sigma}}(s) = \lambda^s_{C_6}g^{-1}_{C_6}(1-s)$.

We have $\lambda_{C_6} = \eta_{\boldsymbol{\sigma}}\eta_{C_6}\eta_{12}$ and

$$\begin{aligned} g_{C_6}(0) &= \tau^0, \\ g_{C_6}(1) = g_{\boldsymbol{\sigma}}(0) &= \eta_{C_6}\eta_{12}\tau^0, \\ g_{\boldsymbol{\sigma}}(1) &= \eta_{\boldsymbol{\sigma}}\eta_{C_6}\eta_{12}\tau^0. \end{aligned} \tag{B23}$$

This represents $2^4 = 16$ different PSGs in class (I)(A) since $\eta_t, \eta_{C_6}, \eta_{\boldsymbol{\sigma}}, \eta_{12} = \pm 1$.

(B) $g_{\boldsymbol{\sigma}}(s)g_{C_6}(1-s) = \mathrm{i}\hat{n}_s\cdot\vec{\tau}$.

Choosing a proper gauge [so that $g_{C_6}(0) = \tau^0$] we have

$$\begin{aligned} g_{C_6}(0) &= \tau^0, \\ g_{C_6}(1) &= \eta_{C_6}\eta_{12}e^{\mathrm{i}\psi_3\tau^3}, \\ g_{\boldsymbol{\sigma}}(0) &= \mathrm{i}\tau^1\eta_{C_6}\eta_{12}e^{-\mathrm{i}\psi_3\tau^3}, \\ g_{\boldsymbol{\sigma}}(1) &= -\mathrm{i}\eta_{\boldsymbol{\sigma}}\eta_{C_6}\eta_{12}e^{\mathrm{i}\psi_3\tau^3}\tau^1, \end{aligned} \tag{B24}$$

where $\psi_3 \equiv 0, \pm 2\pi/3$ stand for the multiples of $2\pi/3$ mod 2π. There are $2^4 \times 3 = 48$ different PSGs in class (I)(B).

(II) $g_{\boldsymbol{T}}(s) = \mathrm{i}\tau^3$.

(i) $\eta_{C_6\boldsymbol{T}} = 1$.

(A) $g_{\boldsymbol{\sigma}}(s) = \lambda^s_{C_6}g^{-1}_{C_6}(1-s)$.

In this case $\lambda_{C6} = \eta_{\boldsymbol{\sigma}}\eta_{C_6}\eta_{12}$, so we have

$$\begin{aligned} g_{C_6}(0) &= \tau^0, \\ g_{\boldsymbol{\sigma}}(0) = g_{C_6}(1) &= \eta_{C_6}\eta_{12}\tau^0, \\ g_{\boldsymbol{\sigma}}(1) &= \eta_{\boldsymbol{\sigma}}\eta_{C_6}\eta_{12}\tau^0. \end{aligned} \tag{B25}$$

There are $2^3 = 8$ different PSGs in class (II)(i)(A).

(B) $g_{\boldsymbol{\sigma}}(s)g_{C_6}(1-s) = \mathrm{i}\hat{n}_s\cdot\vec{\tau}$.

(α) $\eta_{\boldsymbol{\sigma}\boldsymbol{T}} = 1$, *i.e.*, $[g_{\boldsymbol{\sigma}}(s), \tau^3] = 0$.

Here we have

$$\begin{aligned} g_{C_6}(0) &= \tau^0, \\ g_{C_6}(1) &= \eta_{C_6}\eta_{12}\tau^0, \\ g_{\boldsymbol{\sigma}}(0) &= -\mathrm{i}\eta_{\boldsymbol{\sigma}}\tau^3, \\ g_{\boldsymbol{\sigma}}(1) &= \mathrm{i}\tau^3. \end{aligned} \tag{B26}$$

There are $2^3 = 8$ different PSGs in class (II)(i)(B)(α).

(β) $\eta_{\boldsymbol{\sigma}\boldsymbol{T}} = -1$, i.e.$\{g_{\boldsymbol{\sigma}}(s), \tau^3\} = 0$.

Here we have

$$\begin{aligned} g_{C_6}(0) &= \tau^0, \\ g_{C_6}(1) &= \eta_{C_6}\eta_{12}e^{\mathrm{i}\psi_3\tau^3}, \\ g_{\boldsymbol{\sigma}}(0) &= -\mathrm{i}\eta_{\boldsymbol{\sigma}}\tau^1, \\ g_{\boldsymbol{\sigma}}(1) &= \mathrm{i}\tau^1. \end{aligned} \tag{B27}$$

There are $2^3 \times 3 = 24$ different PSGs in class (II)(i)(B)(β) since $\psi_3 = 0, \pm 2\pi/3$.

(ii) $\eta_{C_6\boldsymbol{T}} = -1$.

(A) $g_{\boldsymbol{\sigma}}(s) = \lambda^s_{C_6}g^{-1}_{C_6}(1-s)$.

Here we must have $\eta_{\boldsymbol{\sigma}\boldsymbol{T}} = -1$, $\lambda_{C_6} = \eta_{\boldsymbol{\sigma}}\eta_{C_6}\eta_{12}$, and

$$\begin{aligned} g_{C_6}(0) &= \mathrm{i}\tau^1, \\ g_{C_6}(1) &= -\mathrm{i}\eta_{C_6}\eta_{12}\tau^1, \\ g_{\boldsymbol{\sigma}}(0) &= \mathrm{i}\eta_{C_6}\eta_{12}\tau^1, \\ g_{\boldsymbol{\sigma}}(1) &= -\mathrm{i}\eta_{\boldsymbol{\sigma}}\eta_{C_6}\eta_{12}\tau^1. \end{aligned} \tag{B28}$$

There are $2^3 = 8$ different PSGs in class (II)(ii)(A).

(B) $g_{\boldsymbol{\sigma}}(s)g_{C_6}(1-s) = \mathrm{i}\hat{n}_s\cdot\vec{\tau}$.

(α) $\eta_{\boldsymbol{\sigma}\boldsymbol{T}} = 1$, *i.e.*$[g_{\boldsymbol{\sigma}}(s), \tau^3] = 0$.

Here we have

$$\begin{aligned} g_{C_6}(0) &= \mathrm{i}\tau^1, \\ g_{C_6}(1) &= -\mathrm{i}\eta_{C_6}\eta_{12}\tau^1e^{\mathrm{i}\psi_3\tau^3}, \\ g_{\boldsymbol{\sigma}}(0) &= \tau^0, \\ g_{\boldsymbol{\sigma}}(1) &= \eta_{\boldsymbol{\sigma}}\tau^0. \end{aligned} \tag{B29}$$

There are $2^3 \times 3 = 24$ different PSGs in class (II)(ii)(B)(α) since $\psi_3 = 0, \pm 2\pi/3$.

(β) $\eta_{\boldsymbol{\sigma}\boldsymbol{T}} = -1$, *i.e.*$\{g_{\boldsymbol{\sigma}}(s), \tau^3\} = 0$.

Here we have

$$\begin{aligned} g_{C_6}(0) &= \mathrm{i}\tau^1, \\ g_{C_6}(1) &= -\mathrm{i}\eta_{C_6}\eta_{12}\tau^1e^{\mathrm{i}\psi_3\tau^3}, \\ g_{\boldsymbol{\sigma}}(0) &= \mathrm{i}\tau^1, \\ g_{\boldsymbol{\sigma}}(1) &= -\mathrm{i}\eta_{\boldsymbol{\sigma}}\tau^1. \end{aligned} \tag{B30}$$

There are $2^3 \times 3 = 24$ different PSGs in class (II)(ii)(B)(β) since $\psi_3 = 0, \pm 2\pi/3$.

To summarize, above are the 160 different (algebraic) PSGs with IGG $= \{\pm\tau^0\}$ on a honeycomb lattice. They represent different Z_2 SL states on a honeycomb lattice, which possess all the symmetries of the honeycomb lattice generated by $\{\boldsymbol{T}, T_1, T_2, \boldsymbol{\sigma}, C_6\}$. We also want to emphasize that any solution to the set of equations (B1)–(B14) may look different, but it will be gauge equivalent to one of these 160 PSGs.

On the other hand, such a (algebraic) PSG really corresponds to a SL if and only if it can be realized by a mean-field ansatz $\{u_{ij}\}$ on a honeycomb lattice.[15] In fact, not all of these algebraic PSGs can be realized by an ansatz. After the time-reveral transformation, the mean field amplitude changes sign:[15] $\boldsymbol{T}(u_{ij}) = -u_{ij}$. Gauge transformation $G_{\boldsymbol{T}}$ must change the sign again:

$$-u_{ij} = G_{\boldsymbol{T}}(i)u_{ij}G_{\boldsymbol{T}}(j)^\dagger. \tag{B31}$$

If in an algebraic PSG, $G_{\boldsymbol{T}}(i) = \tau^0$ independent of site, u_{ij} must vanish.

Clearly at least 32 algebraic PSGs among the total 160 types cannot be realized by any mean-field ansatz $\{u_{ij}\}$. These are the PSGs with $G_{\boldsymbol{T}}(i) = g_{\boldsymbol{T}}(s) = \tau^0$ in the class (I)(I)(A) and (B). Since under time reversion $\boldsymbol{T}$ we require $-u_{ij} = G_{\boldsymbol{T}}(i)u_{ij}G_{\boldsymbol{T}}^{\dagger}(j) = u_{ij}$, this leads to the vanishing of all bonds $\{u_{ij} \equiv 0\}$ in the mean-field ansatz. Therefore, there are at the most 128 possible Z_2 SLs that can be realized by a mean-field ansatz on a honeycomb lattice.

APPENDIX C: CLASSIFICATION OF Z_2 PROJECTIVE SYMMETRY GROUPS AROUND U-RVB ANSATZ

In this appendix we focus on those Z_2 SLs near the u-RVB state, which is discussed in Section III. These Z_2 SLs are plausibly connected to a semimetal through a continuous phase transition. The u-RVB state is realized by the following ansatz:

$$u_{ij} = (-1)^{s_i}\,\mathrm{i}\,\chi\tau^0. \tag{C1}$$

Its mean-field bond is nonzero only between nearest neighbors $\langle ij\rangle$, which have different sublattice indices $s_i = 1 - s_j$. By definition, its PSG has the following form:

$$\begin{aligned} G_{T_1}(x_1,x_2,s) &= g_1,\\ G_{T_2}(x_1,x_2,s) &= g_2,\\ G_{\boldsymbol{T}}(x_1,x_2,s) &= (-1)^s g_{\boldsymbol{T}},\\ G_{C_6}(x_1,x_2,s) &= (-1)^s g_{C_6},\\ G_{\boldsymbol{\sigma}}(x_1,x_2,s) &= (-1)^s g_{\boldsymbol{\sigma}}, \end{aligned} \tag{C2}$$

where $g_1,g_2,g_{\boldsymbol{T}},g_{C_6},g_{\boldsymbol{\sigma}} \in \mathrm{SU}(2)$. To find those Z_2 SLs around such a u-RVB state, we need to trace those PSGs with IGG $= \{\pm\tau^0\}$ that looks like Eq. (C2). Consistent conditions (B1)–(B14) now correspond to constraints on the SU(2) matrices $\{g_1,g_2,g_{\boldsymbol{T}},g_{C_6},g_{\boldsymbol{\sigma}}\}$:

$$\begin{gathered} g_1^{-1}g_2^{-1}g_1g_2 = \xi_{12}\tau^0, g_{\boldsymbol{T}}^2 = \xi_{\boldsymbol{T}}\tau^0,\\ g_1^{-1}g_{\boldsymbol{T}}^{-1}g_1g_{\boldsymbol{T}} = \xi_{1\boldsymbol{T}}\tau^0, g_2^{-1}g_{\boldsymbol{T}}^{-1}g_2g_{\boldsymbol{T}} = \xi_{2\boldsymbol{T}}\tau^0,\\ g_2^{-1}g_{C_6}g_1g_{C_6}^{-1} = \xi_{C_61}\tau^0, g_1^{-1}g_{C_6}g_1g_2^{-1}g_{C_6}^{-1} = \xi_{C_62}\tau^0,\\ g_{\boldsymbol{T}}^{-1}g_{C_6}^{-1}g_{\boldsymbol{T}}g_{C_6} = \xi_{C_6\boldsymbol{T}}\tau^0, g_{C_6}^6 = \xi_{C_6}\tau^0,\\ g_1^{-1}g_{\boldsymbol{\sigma}}g_1g_{\boldsymbol{\sigma}}^{-1} = \xi_{\sigma 1}\tau^0, g_2^{-1}g_{\boldsymbol{\sigma}}g_1g_2^{-1}g_{\boldsymbol{\sigma}}^{-1} = \xi_{\sigma 2}\tau^0,\\ g_{\boldsymbol{\sigma}}g_{C_6}g_{\boldsymbol{\sigma}}g_{C_6} = \xi_{\sigma C_6}\tau^0, g_{\boldsymbol{T}}^{-1}g_{\boldsymbol{\sigma}}^{-1}g_{\boldsymbol{T}}g_{\boldsymbol{\sigma}} = \xi_{\sigma\boldsymbol{T}}\tau^0,\\ g_{\boldsymbol{\sigma}}^2 = \xi_{\sigma}\tau^0, \end{gathered} \tag{C3}$$

where all ξ's take values of ± 1. Again, as discussed in Appendix B, we can always make $\xi_{C_61} = \xi_{C_62} = 1$ by choosing a proper gauge. After solving Eqs. (C3), we find that there are 24 gauge-inequivalent solutions in total, as summarized in Table I. In other words, there are 24 different Z_2 SLs around the u-RVB state, suggesting that they are promising candidates of the SL connected to a semimetal on a honeycomb lattice through a continuous phase transition.

APPENDIX D: CONSISTENT CONDITIONS ON THE MEAN-FIELD ANSATZ $\{u_{ij}\}$ ON A HONEYCOMB LATTICE

In this appendix we derive the consistent conditions on an arbitrary mean-field bond u_{ij}, which realizes a SL with a certain PSG on a honeycomb lattice. The basic idea is to find all possible SG elements that transform the two lattice sites $\{i,j\}$ into themselves $\{i,j\}$ or into each other $\{j,i\}$, so that the corresponding PSG elements must transform mean-field bond u_{ij} into itself u_{ij} or its Hermitian conjugate $u_{ij}^{\dagger} = u_{ji}$.

As a special case, identity element 1 always transforms a bond into itself: Correspondingly in a PSG the IGG elements (e.g., τ^0 for a Z_2 ansatz) always transform any bond u_{ij} into itself. This is nothing but the definition of the IGG.

Now we need to look at nontrivial SG elements which transform two lattice sites (connected by the bond) into themselves or into each other. Without loss of generality, we consider the following bond:

$$\langle x_1,x_2,s\rangle \equiv u_{(x_1,x_2,s)(0,0,0)} \tag{D1}$$

1. Regarding time reversal $\boldsymbol{T}$

Any element of the SG can be written as

$$U = \boldsymbol{T}^{\nu_{\boldsymbol{T}}}\cdot T_1^{\nu_{T_1}}\cdot T_2^{\nu_{T_2}}\cdot\boldsymbol{\sigma}^{\nu_{\boldsymbol{\sigma}}}\cdot C_6^{\nu_{C_6}}. \tag{D2}$$

First we study the consistent conditions from time-reversal transformation $\boldsymbol{T}$ and then turn to other group elements.

Notice that time reversal $\boldsymbol{T}$ does not change anything except the sign of the bond,

$$G_{\boldsymbol{T}}(i)u_{ij}[G_{\boldsymbol{T}}(j)]^{\dagger} = -u_{ij}, \tag{D3}$$

so this bond must satisfy the following constraint:

$$G_{\boldsymbol{T}}(x_1,x_2,s)\langle x_1,x_2,s\rangle = -\langle x_1,x_2,s\rangle G_{\boldsymbol{T}}(0,0,0). \tag{D4}$$

2. Conditions on a bond within the same sublattice: $s = 0$

First we study the $s = 0$ case, i.e., a bond within the same sublattice. Since both mirror reflection $\boldsymbol{\sigma}$ and $\pi/3$ rotation C_6 will change the sublattice index s while the translations T_1,T_2 do not, we must have an even number of reflections and rotations, i.e., $\nu_{\boldsymbol{\sigma}} + \nu_{C_6} = 0 \bmod 2$, to transform the bond to itself (or its Hermitian conjugate).

From relations (A22) it is easy to check the five nontrivial elements consisting of $\{\boldsymbol{\sigma},C_6\}$:

$$\begin{aligned} C_6^2(x_1,x_2,0) &= (1-x_1-x_2,x_1,0),\\ C_6^{-2}(x_1,x_2,0) &= (x_2,1-x_1-x_2,0),\\ \boldsymbol{\sigma}C_6(x_1,x_2,0) &= (x_1,1-x_1-y_1,0),\\ \boldsymbol{\sigma}C_6^3(x_1,x_2,0) &= (1-x_1-x_2,x_2,0),\\ \boldsymbol{\sigma}C_6^{-1}(x_1,x_2,0) &= (x_2,x_1,0). \end{aligned} \tag{D5}$$

For the bond to go back after some translations, it is straightforward to find all the consistent conditions on such a bond:

$$\begin{gathered} T_2^{-1}\boldsymbol{\sigma}C_6 : \langle -2x,x,0\rangle \to \langle -2x,x,0\rangle,\\ T_2^{x-1}\boldsymbol{\sigma}C_6 : \langle 0,x,0\rangle \to \langle 0,x,0\rangle^{\dagger},\\ T_1^{-1}\boldsymbol{\sigma}C_6^3 : \langle x,-2x,0\rangle \to \langle x,-2x,0\rangle, \end{gathered}$$

$$T_1^{x-1}\boldsymbol{\sigma}C_6^3 : \langle x,0,0\rangle \to \langle x,0,0\rangle^\dagger, \quad \text{(D6)}$$
$$\boldsymbol{\sigma}C_6^{-1} : \langle x,x,0\rangle \to \langle x,x,0\rangle,$$
$$T_1^x T_2^{-x}\boldsymbol{\sigma}C_6^{-1} : \langle x,-x,0\rangle \to \langle x,-x,0\rangle^\dagger,$$

for $\forall x \in \mathbb{Z}$.

3. Conditions on a bond connecting different sublattices: $s = 1$

In the $s = 1$ case, such a bond connects different sublattices. So only an even number of reflections and rotations, i.e., $\nu_{\boldsymbol{\sigma}} + \nu_{C_6} = 0 \bmod 2$, might transform the bond to itself, while an odd number of reflections and rotations, i.e., $\nu_{\boldsymbol{\sigma}} + \nu_{C_6} = 1 \bmod 2$, can transform the bond $\langle x_1,x_2,1\rangle$ into its Hermitian conjugate $\langle x_1,x_2,1\rangle^\dagger$.

It is straightforward to obtain the following conditions on the bond $\langle x_1,x_2,1\rangle \equiv u_{(x_1,x_2,1)(0,0,0)}$:

$$\boldsymbol{\sigma} : \langle -2x,x,1\rangle \to \langle -2x,x,1\rangle^\dagger,$$
$$\boldsymbol{\sigma}C_6^{-1} : \langle x+1,x,1\rangle \to \langle x+1,x,1\rangle,$$
$$T_1^{-2x-2}T_2^{x+1}\boldsymbol{\sigma}C_6^{-2} : \langle -2x-1,x,1\rangle \to \langle -2x-1,x,1\rangle^\dagger,$$
$$T_1^{x_1-1}T_2^{x_2}C_6^3 : \langle x_1,x_2,1\rangle \to \langle x_1,x_2,1\rangle^\dagger, \quad \text{(D7)}$$
$$T_1^{-1}\boldsymbol{\sigma}C_6^3 : \langle x,-2x,1\rangle \to \langle x,-2x,1\rangle,$$
$$T_1^{x-1}T_2^{x-1}\boldsymbol{\sigma}C_6^2 : \langle x+1,x,1\rangle \to \langle x+1,x,1\rangle^\dagger,$$
$$T_2^{-1}\boldsymbol{\sigma}C_6 : \langle -2x-1,x,1\rangle \to \langle -2x-1,x,1\rangle,$$

for $\forall x,x_1,x_2 \in \mathbb{Z}$.

4. An example: Mean-field ansatz $\{u_{ij}\}$ of Z_2 spin liquids near u-RVB state

To demonstrate the above consistent conditions, let's take a look at how they determine the mean-field ansatz $\{u_{ij}\}$ of any Z_2 SL near the u-RVB state, with PSG generators (C2).

Considering time reversion $\boldsymbol{T}$ we immediately have

$$g_{\boldsymbol{T}}\langle x_1,x_2,s\rangle = -(-1)^s\langle x_1,x_2,s\rangle g_{\boldsymbol{T}}. \quad \text{(D8)}$$

In other words, the bond connecting two sites belonging to the same (different) sublattice(s) anticommutes (commutes) with $g_{\boldsymbol{T}}$.

For the nearest neighbor (n.n.) bond (see Fig. 3) $u_\alpha \equiv \langle 0,0,1\rangle$ we have $x_1 = x_2 = 0, s = 1$. Conditions (D7) and (D8) immediately lead to

$$[u_\alpha, g_{\boldsymbol{T}}] = 0,$$
$$g_{\boldsymbol{\sigma}}u_\alpha = -u_\alpha^\dagger g_{\boldsymbol{\sigma}}, \quad \text{(D9)}$$
$$g_1^{-1}g_{C_6}^3 u_\alpha = -u_\alpha^\dagger g_1^{-1}g_{C_6}^3.$$

For the second n.n. bond $u_\beta \equiv \langle 0,1,0\rangle$, we have $x_1 = 0 = s, x_2 = 1$, and conditions (D6) and (D8) lead to

$$\{u_\beta, g_{\boldsymbol{T}}\} = 0, \quad g_{\boldsymbol{\sigma}}g_{C_6}u_\beta = u_\beta^\dagger g_{\boldsymbol{\sigma}}g_{C_6}. \quad \text{(D10)}$$

For the third n.n. bond $u_\gamma \equiv \langle 1,0,1\rangle$, we have $x_2 = 0, x_1 = s = 1$. Conditions (D7) and (D8) lead to

$$[u_\gamma, g_{\boldsymbol{T}}] = 0,$$
$$g_{C_6}^3 u_\gamma = -u_\gamma^\dagger g_{C_6}^3, \quad \text{(D11)}$$
$$g_{\boldsymbol{\sigma}}g_{C_6}^{-1}u_\gamma = u_\gamma g_{\boldsymbol{\sigma}}g_{C_6}^{-1}.$$

Constraints on further neighbors, e.g., fourth n.n. $\langle 0,1,1\rangle$, fifth n.n. $\langle 1,1,0\rangle$, and sixth n.n. $\langle 2,0,0\rangle$ can be similarly obtained.

APPENDIX E: A SEARCH OF GAPPED SPIN LIQUIDS NEAR THE u-RVB STATE

In Appendix C we showed that there are at most 24 Z_2 SLs around the u-RVB state, which are likely to connect with a semimetal through a continuous phase transition. In this appendix we search for those states with spectral gaps among the 24 SL ansätze. In the end we find out that most of the 24 states are gapless. More specifically, they cannot open up a mass gap through any perturbation around the u-RVB state, which has two graphene-like Dirac cones in the first Brillouin zone. It turns out that only 4 of them, i.e., numbers 16,17,19, and 22 in Table I, are gapped SLs near the u-RVB state.

1. Symmetry-allowed masses in a graphene-like u-RVB state

We start from the low-energy effective Hamiltonian of the u-RVB state, which is described by a massless eight-component Dirac equation. These eight components contain two spin indices (labeled by Pauli matrices $\{\tau^i\}$), two sublattice indices (labeled by Pauli matrices $\{\mu^i\}$), and two valley indices (labeled by Pauli matrices $\{\nu^i\}$). Just like graphene, the two valleys are located at $\mathbf{K}$ and $\mathbf{K}'$, i.e., the vertices in the honeycomb-shaped first Brillouin zone. Following the convention shown in Fig. 1, the momenta of these two cones are $\mathbf{K} = \frac{4\pi}{3}\vec{b}_1 + \frac{2\pi}{3}\vec{b}_2$ and $\mathbf{K}' = \frac{2\pi}{3}\vec{b}_1 + \frac{4\pi}{3}\vec{b}_2$, respectively, where $\{\vec{b}_1 = (\sqrt{3},-1)/\sqrt{3}a, \vec{b}_2 = (0,2)/\sqrt{3}a\}$ are the reciprocal lattice vectors corresponding to lattice vectors $\{\vec{a}_1 = (a,0), \vec{a}_2 = (1,\sqrt{3})a/2\}$.

Expanding the mean-field Hamiltonian of a u-RVB state with $u_\alpha = \mathrm{i}\tau^0$ (here $\mathbf{k} = \frac{2}{\sqrt{3}a}(k_x,k_y) = k_1\vec{b}_1 + k_2\vec{b}_2$),

$$H_{\mathrm{uRVB}} = \mathrm{i}(\psi_{\mathbf{k},A}^\dagger, \psi_{\mathbf{k},B}^\dagger),$$
$$\begin{bmatrix} 0 & -\tau^0(1+e^{-\mathrm{i}k_2}+e^{\mathrm{i}(k_1-k_2)}) \\ \tau^0(1+e^{\mathrm{i}k_2}+e^{\mathrm{i}(k_2-k_1)}) & 0 \end{bmatrix}$$
$$\cdot \begin{pmatrix} \psi_{\mathbf{k},A} \\ \psi_{\mathbf{k},B} \end{pmatrix}$$

around $\mathbf{K}$ and $\mathbf{K}'$, we immediately obtain the Dirac equations

$$H_{\mathbf{K}} = (\psi_{\mathbf{k},A}^\dagger, \psi_{\mathbf{k},B}^\dagger)\begin{bmatrix} 0 & \tau^0(k_y+\mathrm{i}k_x) \\ \tau^0(k_y-\mathrm{i}k_x) & 0 \end{bmatrix}\begin{pmatrix} \psi_{\mathbf{k},A} \\ \psi_{\mathbf{k},B} \end{pmatrix},$$
$$H_{\mathbf{K}'} = (\psi_{\mathbf{k}',A}^\dagger, \psi_{\mathbf{k}',B}^\dagger)\begin{bmatrix} 0 & \tau^0(k'_y-\mathrm{i}k'_x) \\ \tau^0(k'_y+\mathrm{i}k'_x) & 0 \end{bmatrix}\begin{pmatrix} \psi_{\mathbf{k}',A} \\ \psi_{\mathbf{k}',B} \end{pmatrix}.$$

Defining the following eight-component spinor,

$$\Psi^T \equiv (\psi_{\mathbf{k},A}^T, \psi_{\mathbf{k},B}^T, \psi_{\mathbf{k}',B}^T, \psi_{\mathbf{k}',A}^T), \quad \text{(E1)}$$

we can write the above effective Hamiltonian of the u-RVB state as

$$H = \Psi^\dagger\mu^3(\mu^2\partial_x + \mu^1\partial_y)\otimes\tau^0\otimes\nu^0\Psi. \quad \text{(E2)}$$

Therefore only those mass terms $M = \mu^3\otimes\tau^a\otimes\nu^b, a,b = 0,1,2,3$ satisfy that $\{H,\Psi^\dagger M\Psi\} = 0$ so that a mass gap can be opened in the Dirac spectrum. In the following

we study how the mass term changes under the action of symmetry transformation such as spin rotations, time reversal $\boldsymbol{T}$, and translations T_1, T_2. The physical symmetry of a SL state realized by the mean-field ansatz allows only those masses that are invariant under the corresponding PSG. If a PSG already rules out all possible mass terms $M = \mu^3 \otimes \tau^a \otimes \nu^b, a,b = 0,1,2,3$, we conclude the corresponding SL realized by the mean-field ansatz is gapless.

First we work out the transformation rules of Dirac spinor Ψ and M under a PSG. We focus on the 24 PSGs near the u-RVB state with form (C2) as summarized in Table I.

a. Spin rotations

It's straightforward to show that a spin rotation along the $\hat{z}$ axis by 2θ angle is realized by

$$\Psi \to e^{\mathrm{i}\theta}\Psi, \tag{E3}$$

while a spin rotation along the $\hat{y}$ axis by π angle is realized by

$$\Psi \to \mathrm{i}\tau^2\mu^1\nu^1\Psi^*. \tag{E4}$$

Apparently S_z rotations leave the mass term invariant, while under S_y rotations by π the mass term transforms in the following way:

$$M \to -\mu^1 \otimes \nu^1 \otimes \tau^2 M^T \tau^2 \otimes \mu^1 \otimes \nu^1. \tag{E5}$$

Since the mass term is invariant under spin rotations, its allowed form as seen from the above constraint can only be

$$M_A^{(a)} = \mu^3 \otimes \nu^3 \otimes \tau^a, \quad a = 1,2,3 \tag{E6}$$

or

$$M_B^{(b)} = \mu^3 \otimes \nu^b \otimes \tau^0, \quad b = 0,1,2. \tag{E7}$$

b. Time reversal T

Since a mean-field bond u_{ij} becomes $-(-1)^{s_i} g_T u_{ij} g_T^\dagger (-1)^{s_j}$ under the time reversal transformation in a PSG (C2), clearly $\boldsymbol{T}$ is realized by

$$\begin{aligned} \Psi &\to g_T^\dagger \otimes \mu^3 \otimes \nu^3 \Psi, \\ M &\to -M, \end{aligned} \tag{E8}$$

so the mass term is invariant under time reversal $\boldsymbol{T}$ if

$$M = -g_T \otimes \mu^3 \otimes \nu^3 M g_T^\dagger \otimes \mu^3 \otimes \nu^3. \tag{E9}$$

Ten SLs near the u-RVB state, i.e., Nos. 1–10 in Table I, have $g_T = \tau^0$. In these cases, mass terms $M_A^{(a)}, a = 1,2,3$ will violate transformation rule (E9), and the only allowed masses are $M_B^{(1)}, M_B^{(2)}$.

The other 14 SLs around the u-RVB state (Nos. 11–24 in Table I) are characterized by $g_T = \mathrm{i}\tau^3$. In this case the allowed masses are $M_B^{(1)}, M_B^{(2)}$ and $M_A^{(1)}, M_A^{(2)}$.

c. Translations T_1, T_2

Under translations T_1, T_2 in a PSG, (C2), the eight-component spinor changes as

$$\begin{aligned} T_1 &: \Psi \to e^{-\mathrm{i}\frac{2\pi}{3}\nu^3} \otimes g_1^\dagger \Psi, \\ T_2 &: \Psi \to e^{\mathrm{i}\frac{2\pi}{3}\nu^3} \otimes g_2^\dagger \Psi, \end{aligned} \tag{E10}$$

since $\mathbf{K} \cdot \vec{a}_{1,2} = \mp\frac{2\pi}{3}$ and $\mathbf{K}' \cdot \vec{a}_{1,2} = \pm\frac{2\pi}{3}$. For the mass term to be invariant,

$$\begin{aligned} M &= e^{\mathrm{i}\frac{2\pi}{3}\nu^3} \otimes g_1 M e^{-\mathrm{i}\frac{2\pi}{3}\nu^3} \otimes g_1^\dagger \\ &= e^{-\mathrm{i}\frac{2\pi}{3}\nu^3} \otimes g_2 M e^{\mathrm{i}\frac{2\pi}{3}\nu^3} \otimes g_2^\dagger, \end{aligned} \tag{E11}$$

the symmetry-allowed masses can only be: $M_B^{(0)}$ and $M_A^{(a)}, a = 1,2,3$ if $g_1 = g_2 = \tau^0$; $M_B^{(0)}$ and $M_A^{(3)}$ if $g_1 = g_2^{-1} = e^{\mathrm{i}2\pi/3\tau^3}$; $M_B^{(0)}$ for the special case of No. 10 in Table I.

Combining conditions (E9) and (E11) we can see that $\{M_B^{(b)}, b = 0,1,2\}$ are not allowed by symmetry in any of the 24 SLs near the u-RVB state. In what follows we will focus on masses $M_A^{(a)}, a = 1,2,3$.

d. Reflection σ

Similar to time reversal $\boldsymbol{T}$, under reflection along the $\hat{x}$ axis, the spinor transforms as

$$\Psi \to \mu^1 \cdot g_{\boldsymbol{\sigma}}^\dagger \otimes \mu^3 \otimes \nu^3 \Psi = -\mathrm{i} g_{\boldsymbol{\sigma}}^\dagger \otimes \mu^2 \otimes \nu^3 \Psi. \tag{E12}$$

The mass term is invariant under reflection $\boldsymbol{\sigma}$ if

$$M = g_{\boldsymbol{\sigma}} \otimes \mu^2 \otimes \nu^3 M g_{\boldsymbol{\sigma}}^\dagger \otimes \mu^2 \otimes \nu^3. \tag{E13}$$

The symmetry-allowed masses are none if $g_{\boldsymbol{\sigma}} = \tau^0$ or $M_A^{(a)}, a \neq b$, if $g_{\boldsymbol{\sigma}} = \mathrm{i}\tau^b$.

e. π/3 rotation C_6

Under C_6, i.e., a rotation by $\pi/3$, the spinor transforms as

$$\Psi \to g_{C_6}^\dagger \otimes e^{\mathrm{i}\frac{5\pi}{6}\mu^3} \otimes \left(\frac{\sqrt{3}}{2}\nu^1 - \frac{1}{2}\nu^2\right)\Psi. \tag{E14}$$

The mass term is invariant under reflection $\boldsymbol{\sigma}$ if

$$\begin{aligned} M = g_{C_6} \otimes e^{-\mathrm{i}\frac{5\pi}{6}\mu^3} \otimes \left(\frac{\sqrt{3}}{2}\nu^1 - \frac{1}{2}\nu^2\right) \cdot M \\ \cdot g_{C_6}^\dagger \otimes e^{\mathrm{i}\frac{5\pi}{6}\mu^3} \otimes \left(\frac{\sqrt{3}}{2}\nu^1 - \frac{1}{2}\nu^2\right). \end{aligned} \tag{E15}$$

The symmetry-allowed masses are none if $g_{C_6} = \tau^0, e^{\mathrm{i}\theta\tau^{1,3}}$ with $\theta \neq 0 \bmod \pi/2$, or $M_A^{(a)}, a \neq b$, if $g_{C_6} = \mathrm{i}\tau^b$.

2. Realizing the four gapped Z_2 spin liquids near the u-RVB state

Among all 24 SLs near the u-RVB states, it turns out that there are no symmetry-allowed masses for 20 of them. In other words, these 20 SLs cannot open up a mass gap through a perturbation around the u-RVB state. Only the following 4 SLs near the u-RVB state can obtain an energy gap in the spectrum through adding a symmetry-allowed mass term:

No. 16 with two symmetry-allowed masses $M_A^{(1,2)} = \mu^3 \otimes \nu^3 \otimes \tau^{1,2}$;

No. 17 with one symmetry-allowed mass $M_A^{(2)} = \mu^3 \otimes \nu^3 \otimes \tau^2$;

No. 19 with one symmetry-allowed mass $M_A^{(2)} = \mu^3 \otimes \nu^3 \otimes \tau^2$;

No. 22 with one symmetry-allowed mass $M_A^{(2)} = \mu^3 \otimes \nu^3 \otimes \tau^2$.

TABLE II. Symmetry-allowed mean-field ansätze of the 4 possible gapped SLs near the u-RVB state. We follow the notation for mean-field bonds in Appendix D. We only summarize the mean-field bonds that are necessary to realize a gapped Z_2 SL. Ellipses represents those longer-range mean-field bonds unnecessary for a Z_2 SL, which are not listed in this table. Up to third n.n. mean-field bonds $\{u_\alpha,u_\beta,u_\gamma\}$, only one Z_2 SL, i.e., No. 19 can be realized on a honeycomb lattice.

No.	u_α	u_β	u_γ	u_δ	u_ε	Ninth n.n. $\langle 1,2,0\rangle$
16	$i\tau^0$	$\{\tau^1,\tau^2\}$	$i\tau^0$	$i\tau^0$	$\{\tau^1,\tau^2\}$	$\cdots$
17	$i\tau^0$	τ^2	$i\tau^0$	$\{i\tau^0,\tau^3\}$	$\cdots$	$\cdots$
19	$\{i\tau^0,\tau^3\}$	$\{\tau^1,\tau^2\}$	$\cdots$	$\cdots$	$\cdots$	$\cdots$
22	$i\tau^0$	τ^2	$i\tau^0$	$i\tau^0$	τ^2	$\{\tau^1,\tau^2\}$

In fact, as summarized in Table II, these 4 gapped SLs can be realized by a mean-field ansatz $\{u_{ij}\}$, which satisfies consistent conditions from the corresponding PSG, as discussed in Appendix D. In the following we describe the mean-field ansatz for these 4 gapped Z_2 SLs. In the end only one gapped Z_2 SL, i.e., No. 19, can be realized by a mean-field ansatz up to third n.n. bonds.

a. Z_2 spin liquid No. 16: Up to fifth n.n. bonds needed

The mean-field ansatz $\{u_{ij}\}$ for Z_2 SL No. 16 is summarized in Table II up to fifth n.n. bonds. The corresponding SL has a Z_2 gauge structure if and only if $[u_\beta,u_\varepsilon]\neq 0$, so that the IGG of this mean-field ansatz is a Z_2 group $\{\pm\tau^0\}$.

It is straightforward to check that the second n.n. bond $u_\beta = \beta_1\tau^1+\beta_2\tau^2$ opens up a mass gap $M\sim\mu^3\otimes\nu^3\otimes(\beta_1\tau^1+\beta_2\tau^2)=\beta_1 M_A^{(1)}+\beta_2 M_A^{(2)}$.

b. Z_2 spin liquid No. 17: Up to fourth n.n. bonds needed

The mean-field ansatz $\{u_{ij}\}$ for Z_2 SL No. 17 is summarized in Table II up to fourth n.n. bonds. The corresponding SL has a Z_2 gauge structure if and only if $[u_\beta,u_\delta]\neq 0$, so that the IGG of this mean-field ansatz is a Z_2 group $\{\pm\tau^0\}$.

It is straightforward to check that the second n.n. bond $u_\beta=\beta\tau^2$ opens up a mass gap $M\sim\beta\mu^3\otimes\nu^3\otimes\tau^2=\beta M_A^{(2)}$.

c. Z_2 spin liquid No. 19: Up to second n.n. bonds needed

The mean-field ansatz $\{u_{ij}\}$ for Z_2 SL No. 17 is summarized in Table II up to second n.n. bonds. The corresponding SL has a Z_2 gauge structure if and only if $u_\beta=\beta_1\tau^1+\beta_2\tau^2$ with $\beta_1,\beta_2\neq 0$, so that the IGG of this mean-field ansatz is a Z_2 group $\{\pm\tau^0\}$. This is the only gapped Z_2 SL near the u-RVB state that can be realized in a mean-field ansatz up to third n.n. bonds.

It is straightforward to check that the second n.n. bond $u_\beta=\beta_1\tau^1+\beta_2\tau^2$ opens up a mass gap $M\sim\beta_2\mu^3\otimes\nu^3\otimes\tau^2=\beta_2 M_A^{(2)}$.

d. Z_2 spin liquid No. 22: Up to ninth n.n. bonds needed

The mean-field ansatz $\{u_{ij}\}$ for Z_2 SL No. 17 is summarized in Table II up to ninth n.n. bonds. The corresponding SL has a Z_2 gauge structure if and only if $[u_\beta,u_9]\neq 0$, so that the IGG of this mean-field ansatz is a Z_2 group $\{\pm\tau^0\}$. $u_9\equiv\langle 1,2,0\rangle$ is the ninth n.n. mean-field bond. In this Z_2 SL, the symmetry-allowed consistent mean-field bonds for the sixth, seventh, and eigth n.n.'s are

$$u_6\equiv\langle 2,0,0\rangle\propto\tau^2,$$
$$u_7\equiv\langle 2,0,1\rangle\propto i\tau^0,$$
$$u_8\equiv\langle 0,2,1\rangle\propto i\tau^0.$$

It is straightforward to check that the second n.n. bond $u_\beta=\beta\tau^2$ opens up a mass gap $M\sim\beta\mu^3\otimes\nu^3\otimes\tau^2=\beta M_A^{(2)}$.

APPENDIX F: SCHWINGER-FERMION MEAN-FIELD STUDY OF THE J_1-J_2 MODEL ON A HONEYCOMB LATTICE

Can a SPS be realized in the Hubbard model when $t/U\sim 1/4$, where numerics show a gapped SL phase? In particular, by the Mott transition theory of Hermele,[23] the u-RVB (or ASL) state is in the neighborhood of the Mott transition. Can a SPS be more favorable than the ASL state? To address this question, we use a t/U expansion of the Hubbard model[43] to obtain an effective J_1-J_2 spin model on a honeycomb lattice:

$$H=J_1\sum_{\langle ij\rangle}\vec{S}_i\cdot S_j+J_2\sum_{\langle\langle ij\rangle\rangle}\vec{S}_i\cdot S_j, \tag{F1}$$

where J_1 and J_2 are the first neighbor and second neighbor AF couplings. Following Ref. 43, we find that, up to t^4/U^3 order, the effective J_1 and J_2 are

$$J_1=4t^2/U-16t^4/U^3,\quad J_2=4t^4/U^3. \tag{F2}$$

Naively plugging in $t/U\sim 1/4$ gives $J_2/J_1\sim 1/12$.

We use the following variationally mean-field ansatz:

$$H_{MF}=\chi\sum_{\langle ij\rangle}f_{i\alpha}^\dagger f_{j\alpha}+\Delta e^{i\theta}\sum_{\langle\langle ij\rangle\rangle\in A}\epsilon_{\alpha\beta}f_{i\alpha}^\dagger f_{j\beta}^\dagger + \Delta e^{-i\theta}\sum_{\langle\langle ij\rangle\rangle\in B}\epsilon_{\alpha\beta}f_{i\alpha}^\dagger f_{j\beta}^\dagger+\text{h.c.} \tag{F3}$$

It is equivalent to SPS ansatz (11) by an SU(2) gauge transformation. Note that this mean-field study is biased toward a spin disordered ground state. For example, we do not include a Néel order which is known to be the ground state at $J_2=0$, and we also do not include the spiral spin order which is found by semiclassical study of the J_1-J_2 model.[44,45] The purpose of the current mean-field study is to understand whether a gapped SL can be more favorable compared with the gapless ASL state when J_2 is tuned up and frustration becomes important.

By minimizing the mean-field energy in Eq. (5), the phase diagram of J_1-J_2 model is obtained and shown in Fig. 4, where we fix $J_1+J_2=1$ and E_{MF} is scaled from Eq. (5) by 8/3. We find that when $J_2/J_1<0.85$ (or $J_2/(J_1+J_2)<0.46$), the ground state is the u-RVB(or ASL) state: $\chi\neq 0$ and $\Delta=0$. When $J_2/J_1>0.85$, the ground state is an s-wave pairing state: $\chi,\Delta\neq 0$, and $\theta=0$. The s-wave pairing state opens an energy gap for spinons but has a remaining $U(1)$ gapless gauge fluctuation. Due to monopole proliferation[38] the s-wave pairing state is not a stable phase. In this mean-field study, the gauge fluctuations are not considered and this is the reason why we find the s-wave pairing state as a ground state. Taking gauge

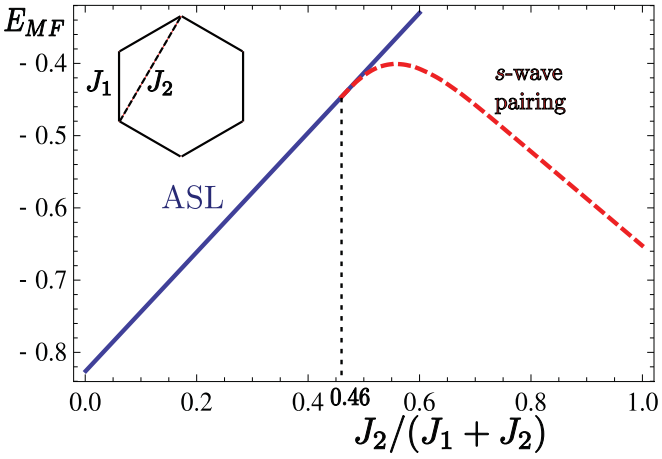

FIG. 4. (Color online) Mean-field phase diagram of $J_1 - J_2$ model by Schwinger-fermion approach.

fluctuations into account, the likely fate of the s-wave pairing state is that θ becomes nonzero and the Z_2 SPS state is realized.

We propose to study the J_1-J_2 model by Gutzwiller projected wave-function variational approach[46] because it can be viewed as a method to include the gauge fluctuation. We leave this projected wave-function study as a direction of future research, which may realize the SPS as the ground state. Projected wave functions are also classified by PSG, so the present work also provides guideline for the search of ground states in the projected wave-function space.

APPENDIX G: DERIVATION OF THE MUTUAL CHERN–SIMONS TERM

We start from the following low-energy effective Lagrangian of spinon fields ψ in imaginary time (i.e., Euclidean space-time):

$$\mathcal{L} = \psi^\dagger \gamma_0(\partial_\mu - i a_\mu)\gamma_\mu \psi + m\, \hat{n}\cdot\psi^\dagger \vec{M}\psi + \frac{1}{4g_a^2} f_{\mu\nu}^2 + \frac{1}{2u}(\partial_\mu \hat{n})^2. \tag{G1}$$

We are aiming for an effective action of gauge fields a_μ obtained by integrating out the spinon fields ψ in

$$\mathcal{L}_{\text{eff}} = \bar{\psi}[\mathrm{i}\gamma_\mu(\partial_\mu - \mathrm{i}a_\mu) + \mathrm{i}m\hat{n}\cdot\vec{\sigma}]\psi \tag{G2}$$

where we define $\bar{\psi} \equiv \psi^\dagger\gamma^0$. For simplicity let's denote $-\mathrm{i}\mathcal{G}^{-1} = \gamma_\mu(\partial_\mu - \mathrm{i}a_\mu) + m\hat{n}\cdot\vec{\sigma}$, then integrate out spinon fields ψ to yield the effective action $\mathcal{S} = -\ln\det(\mathcal{G}^{-1}) = -\mathrm{Tr}\ln(\mathcal{G}^{-1})$. Following the spirit of Abanov and Wiegmann,[26,47] we use a large-m expansion to obtain the low-energy effective theory in the long-wavelength limit $\omega \ll m$. By defining $\mathcal{G}_0^{-1} = \mathrm{i}(\gamma_\mu\partial_\mu + m\hat{n}\cdot\vec{\sigma})$ we have $\mathcal{G}^{-1} = \mathcal{G}_0^{-1} + a_\mu\gamma_\mu$. Let's denote $\not{\partial} \equiv \gamma_\mu\partial_\mu$ and similarly $\not{a} \equiv \gamma_\mu a_\mu$, and we have

$$\mathcal{S} = -\mathrm{Tr}\ln(\mathcal{G}_0^{-1} + \not{a}) = -\mathrm{Tr}\ln(\mathcal{G}_0^{-1}) - \mathrm{Tr}\ln(1 + \mathcal{G}_0\not{a}) = \mathcal{S}_0 + \sum_{l=1}^{\infty}(-1)^l \mathrm{Tr}(\mathcal{G}_0\not{a})^l.$$

Here $\mathcal{S}_0$ gives the nonlinear-sigma-model dynamics $\sim(\partial_\mu\hat{n})^2$ of vector $\hat{n}$, while the coupling between vector $\hat{n}$ and gauge field a_μ is given by the second term. In the large-m expansion we consider only the leading-order term:

$$\mathcal{S}_1 = -\mathrm{Tr}(\mathcal{G}_0\not{a}) = -\mathrm{Tr}\{\mathcal{G}_0^{-1}[\mathcal{G}_0^{-1}(\mathcal{G}_0^{-1})^\dagger]^{-1}\not{a}\}.$$

It is straightforward to check that $\mathcal{G}_0^{-1}(\mathcal{G}_0^{-1})^\dagger = -\partial^2 + m^2 - m\vec{\sigma}\cdot\not{\partial}\hat{n}$; therefore large-$m$ expansion leads to

$$[\mathcal{G}_0^{-1}(\mathcal{G}_0^{-1})^\dagger]^{-1} = (-\partial^2 + m^2)^{-1}\sum_{l=0}^{\infty}\left(\frac{m\vec{\sigma}\cdot\not{\partial}\hat{n}}{-\partial^2+m^2}\right)^l,$$

and consequently

$$\mathcal{S}_1 = -\sum_{l=0}^{\infty}\mathrm{Tr}\left\{\frac{\mathrm{i}(\not{\partial} + m\hat{n}\cdot\vec{\sigma})}{-\partial^2+m^2}\left(\frac{m\vec{\sigma}\cdot\not{\partial}\hat{n}}{-\partial^2+m^2}\right)^l\not{a}\right\}.$$

It turns out that $l = 0, 1$ terms both vanish and the leading-order correction to the low-energy effective action is the following topological term:

$$\mathcal{S}_{\text{topo}} = -a_\mu\mathrm{Tr}\left[\gamma_\mu\frac{\mathrm{i}m\hat{n}\cdot\vec{\sigma}}{-\partial^2+m^2}\left(\frac{m\gamma_\nu(\partial_\nu\hat{n})\cdot\vec{\sigma}}{-\partial^2+m^2}\right)^2\right] = \frac{\mathrm{i}}{4\pi}\epsilon_{\mu\nu\lambda}a_\mu\hat{n}\cdot(\partial_\nu\hat{n}\times\partial_\lambda\hat{n}). \tag{G3}$$

Notice that in the CP^1 parametrization of order parameter $\hat{n} = w^\dagger\sigma w$, spinor w is the eigenvector of $\hat{n}\cdot\vec{\sigma}$ whose spin orientation is along unit vector $\hat{n}$. Therefore the skyrmion current of $\hat{n}$,

$$J_\mu^{Sk} = \frac{1}{2}\cdot\frac{1}{4\pi}\epsilon_{\mu\nu\lambda}\hat{n}\cdot(\partial_\nu\hat{n}\times\partial_\lambda\hat{n}), \tag{G4}$$

which equals half the winding number of $\hat{n}$ wrapping around S^2, is nothing but the Berry's phase[48] for spinor w. Since spinor w obtains the π phase (i.e., a minus sign) as $\hat{n}$ wraps around S^2 once (i.e., $\hat{n}$ covers 4π solid angle), this gives a direct correspondence between the skyrmion current density and the $U(1)$ gauge field strength $F_{\mu\nu}$ coupled to w:

$$\frac{1}{4\pi}\epsilon_{\mu\nu\lambda}\hat{n}\cdot(\partial_\nu\hat{n}\times\partial_\lambda\hat{n}) = \frac{1}{\pi}\epsilon_{\mu\nu\lambda}\partial_\nu A_\lambda. \tag{G5}$$

Therefore topological term (G3) is exactly the mutual CS term mentioned earlier

$$\mathcal{S}_{\text{topo}} = \frac{\mathrm{i}}{\pi}\epsilon_{\mu\nu\lambda}a_\mu\partial_\nu A_\lambda.$$

[1] Y. Shimizu, K. Miyagawa, K. Kanoda, M. Maesato, and G. Saito, Phys. Rev. Lett. **91**, 107001 (2003).
[2] T. Itou, A. Oyamada, S. Maegawa, M. Tamura, and R. Kato, Phys. Rev. B **77**, 104413 (2008).
[3] M. Yamashita, N. Nakata, Y. Senshu, M. Nagata, H. M. Yamamoto, R. Kato, T. Shibauchi, and Y. Matsuda, Science **328**, 1246 (2010).
[4] P. Anderson, Mater. Res. Bull. **8**, 153 (1973).
[5] M. Oshikawa and T. Senthil, Phys. Rev. Lett. **96**, 060601 (2006).
[6] N. Read and S. Sachdev, Phys. Rev. Lett. **66**, 1773 (1991).
[7] R. Moessner and S. L. Sondhi, Phys. Rev. Lett. **86**, 1881 (2001).

[8]X.-G. Wen, Phys. Rev. Lett. **90**, 016803 (2003).
[9]A. Kitaev, Ann. Phys. **321**, 2 (2006).
[10]O. I. Motrunich, Phys. Rev. B **72**, 045105 (2005).
[11]S.-S. Lee and P. A. Lee, Phys. Rev. Lett. **95**, 036403 (2005).
[12]Z. Y. Meng, T. C. Lang, S. Wessel, F. F. Assaad, and A. Muramatsu, Nature (London) **464**, 847 (2010).
[13]F. Wang, Phys. Rev. B **82**, 024419 (2010).
[14]C. Xu and S. Sachdev, Phys. Rev. Lett. **105**, 057201 (2010).
[15]X.-G. Wen, Phys. Rev. B **65**, 165113 (2002).
[16]G. Baskaran, Z. Zou, and P. W. Anderson, Solid State Commun. **63**, 973 (1987).
[17]G. Kotliar and J. Liu, Phys. Rev. B **38**, 5142 (1988).
[18]I. Affleck, Z. Zou, T. Hsu, and P. W. Anderson, Phys. Rev. B **38**, 745 (1988).
[19]X.-G. Wen and P. A. Lee, Phys. Rev. Lett. **76**, 503 (1996).
[20]D. P. Arovas and A. Auerbach, Phys. Rev. B **38**, 316 (1988).
[21]C. Gros, R. Joynt, and T. M. Rice, Phys. Rev. B **36**, 381 (1987).
[22]S. Florens and A. Georges, Phys. Rev. B **70**, 035114 (2004).
[23]M. Hermele, Phys. Rev. B **76**, 035125 (2007).
[24]Y. Ran, A. Vishwanath, and D.-H. Lee, e-print arXiv:0806.2321v2 (2008).
[25]T. Grover and T. Senthil, Phys. Rev. Lett. **100**, 156804 (2008).
[26]A. G. Abanov and P. B. Wiegmann, Nucl. Phys. B **570**, 685 (2000).
[27]T. H. Hansson, V. Oganesyan, and S. L. Sondhi, Ann. Phys. **313**, 497 (2004).
[28]S.-P. Kou, M. Levin, and X.-G. Wen, Phys. Rev. B **78**, 155134 (2008).
[29]A. V. Chubukov, T. Senthil, and S. Sachdev, Phys. Rev. Lett. **72**, 2089 (1994).
[30]A. V. Chubukov, S. Sachdev, and T. Senthil, Nucl. Phys. B **426**, 601 (1994).
[31]S. V. Isakov, T. Senthil, and Y. B. Kim, Phys. Rev. B **72**, 174417 (2005).
[32]L. Seehofer, G. Falkenberg, and R. Johnson, Surf. Sci. **290**, 15 (1993).
[33]S. Cahangirov, M. Topsakal, E. Akturk, H. Sahin, and S. Ciraci, Phys. Rev. Lett. **102**, 236804 (2009).
[34]L.-M. Duan, E. Demler, and M. D. Lukin, Phys. Rev. Lett. **91**, 090402 (2003).
[35]R. Jordens, N. Strohmaier, K. Gunter, H. Moritz, and T. Esslinger, Nature (London) **455**, 204 (2008).
[36]F. J. Wegner, J. Math. Phys. **12**, 2259 (1971).
[37]J. B. Kogut, Rev. Mod. Phys. **51**, 659 (1979).
[38]A. M. Polyakov, Nucl. Phys. B **120**, 429 (1977).
[39]T. Appelquist and D. Nash, Phys. Rev. Lett. **64**, 721 (1990).
[40]D. J. Gross and F. Wilczek, Phys. Rev. Lett. **30**, 1343 (1973).
[41]H. D. Politzer, Phys. Rev. Lett. **30**, 1346 (1973).
[42]T. Senthil, A. Vishwanath, L. Balents, S. Sachdev, and M. P. A. Fisher, Science **303**, 1490 (2004).
[43]A. H. MacDonald, S. M. Girvin, and D. Yoshioka, Phys. Rev. B **37**, 9753 (1988).
[44]E. Rastelli, A. Tassi, and L. Reatto, Physica B + C **97**, 1 (1979).
[45]J. Fouet, P. Sindzingre, and C. Lhuillier, Eur. Phys. J. B **20**, 241 (2001).
[46]C. Gros, Ann. Phys. **189**, 53 (1989).
[47]A. G. Abanov and P. B. Wiegmann, J. High Energy Phys. **2001**, 030 (2001).
[48]M. V. Berry, Proc. R. Soc. London Ser. A **392**, 45 (1984).
[49]P. A. Lee, N. Nagaosa, T.-K. Ng, and X.-G. Wen, Phys. Rev. B **57**, 6003 (1998).